Forecasting of the Upper Atmosphere via Assimilation of Electron Density Data

Timothy Kodikara

DLR

Outline

- The Study
- TIE-GCM
- Data Assimilation
- Results
- Validation of the Forecasts
- Impact on the Thermosphere
- Summary and Conclusions

The Study

This study presents results from experiments of driving a physics-based thermosphere model (TIE-GCM) by assimilating radio occultation electron density (*Ne*) profiles from the joint USA-Taiwan Constellation Observing System for Meteorology, Ionosphere and Climate/Formosa Satellite 3 (COSMIC/FORMOSAT-3; hereinafter COSMIC) mission using an ensemble Kalman filter.

This study not only helps to gauge the accuracy of the assimilation, to explain the inherent model bias, and to understand the limitations of the framework, but it also demonstrates the capability of the assimilation technique to forecast the highly dynamical thermosphere in the presence of **realistic** data assimilation scenarios.

Thermosphere Ionosphere Electrodynamics-General Circulation Model

Magnetic activity
High-lat input
(Kp, IMF)

Solar EUV/FUV
($F_{10.7}$)

Lower atm forcing (tides)
(GSWM, Eddy Diffusion)

Configuration used in this study

$F_{10.7}$ based EUVAC;
Solomon & Qian, 2005;

GSWM, Hagan et al., 1999
Eddy, Qian et al., 2009

Heelis et al., 1982;
Weimer 2005;
AMIE (data assimilation);
LFM magnetosphere

TIE-GCM

Latitude x Longitude:
2.5° × 2.5° or 5° × 5°
Height: 29 or 57
constant pressure levels

Low/mid lat electrodynamics:
neutral wind dynamo in
geo-mag apex coordinates.
Richmond et al., 1992; 1995

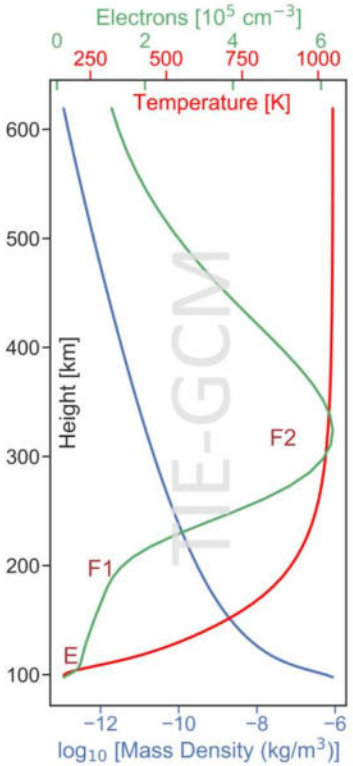

Neutral Density,
Composition,
Temperature,
Winds,Energy,
Ionosphere (Ne,
TEC), ...

NCAR UCAR HAO

Developed by the High Altitude Observatory, Colorado, USA

Data Assimilation – Ensemble Kalman Filter

NCAR's
Data
Assimilation
Research
Testbed

DART parameters (ensemble size, localisation, assimilation window,...)

Assimilate the obs using the EnKF

State vector

$$\boldsymbol{x} = [\boldsymbol{\psi}^{Tn}; \boldsymbol{\psi}^{\gamma O}; \boldsymbol{\psi}^{\gamma O^+}; \boldsymbol{\psi}^{\gamma O_2}; \boldsymbol{\psi}^{U}; \boldsymbol{\psi}^{V}; \boldsymbol{\psi}^{Ne}].$$

Advance the model

Diagnostics: explore state before and after assimilation cycle

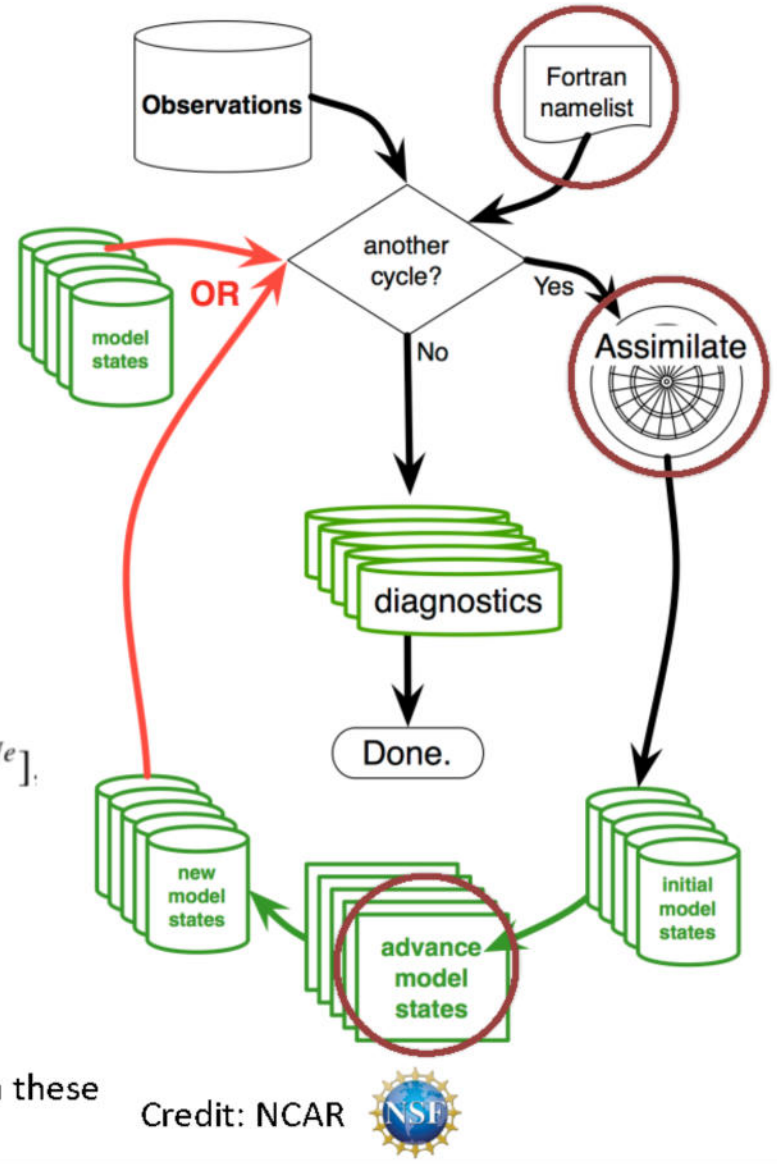

Integrated the latest TIE-GCM into DART to perform these experiments

Credit: NCAR

Results from Experiments E1 and E2

- E1: Assimilate COSMIC-*Ne* during **solar minimum** (2008 March 4–8)
- E2: Assimilate COSMIC-*Ne* during **solar maximum** (2014 June 2–6)

Description of the next three figures:

The number of COSMIC-*Ne* profiles available to assimilate significantly depends on latitude and local time. The following three figures show the root mean square error (RMSE) for E1 relative to COSMIC-*Ne* observations at six different altitude regions with a width of 50 km extending from 150 to 450 km. Each Figure is for a specific latitude region. The results are averaged hourly by local time (LT).

The number of assimilated observations per LT-bin is marked in **green**. The gaps in the lines indicate the unavailability of observations to represent the respective LT in the specified latitude-altitude region. The **TIE-GCM** run is driven by using daily geophysical indices (F10.7, Kp). The **forecast** here is a forecast with a lead time of one hour. The **analysis** is the state after assimilation. As the assimilation progresses, the forecast run uses the analysis state from the previous time step to compute the expected state of the current time step. For example, the forecast state at 2 UT used the analysis state at 1 UT as the base state to drive the model forward by 1 hour.

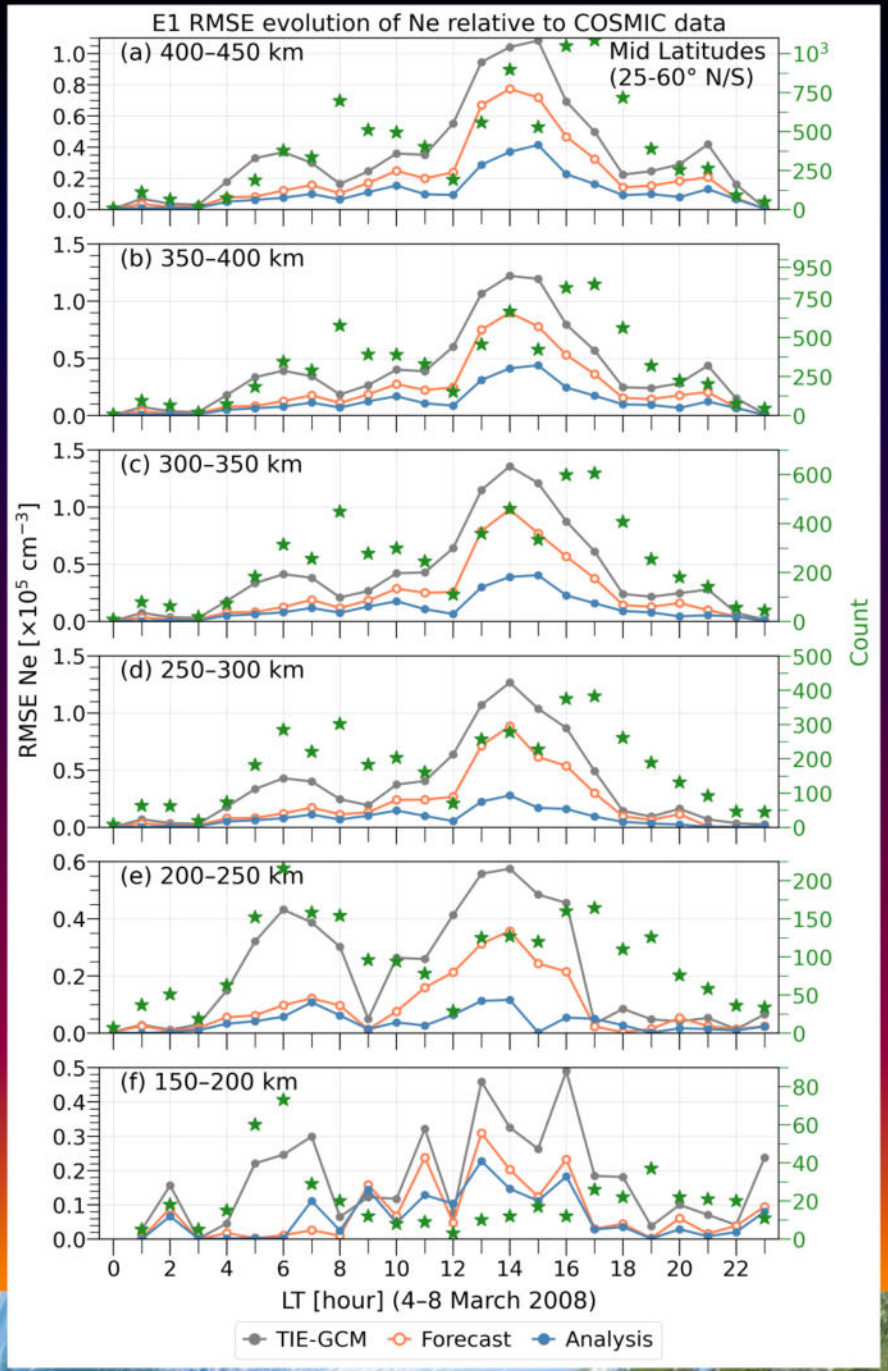
E1 RMSE evolution of Ne relative to COSMIC data
(a) 400–450 km
Mid Latitudes
(25-60° N/S)
(b) 350–400 km
(c) 300–350 km
(d) 250–300 km
(e) 200–250 km
(f) 150–200 km
RMSE Ne [×10^5 cm^-3]
Count
LT [hour] (4–8 March 2008)
TIE-GCM
Forecast
Analysis

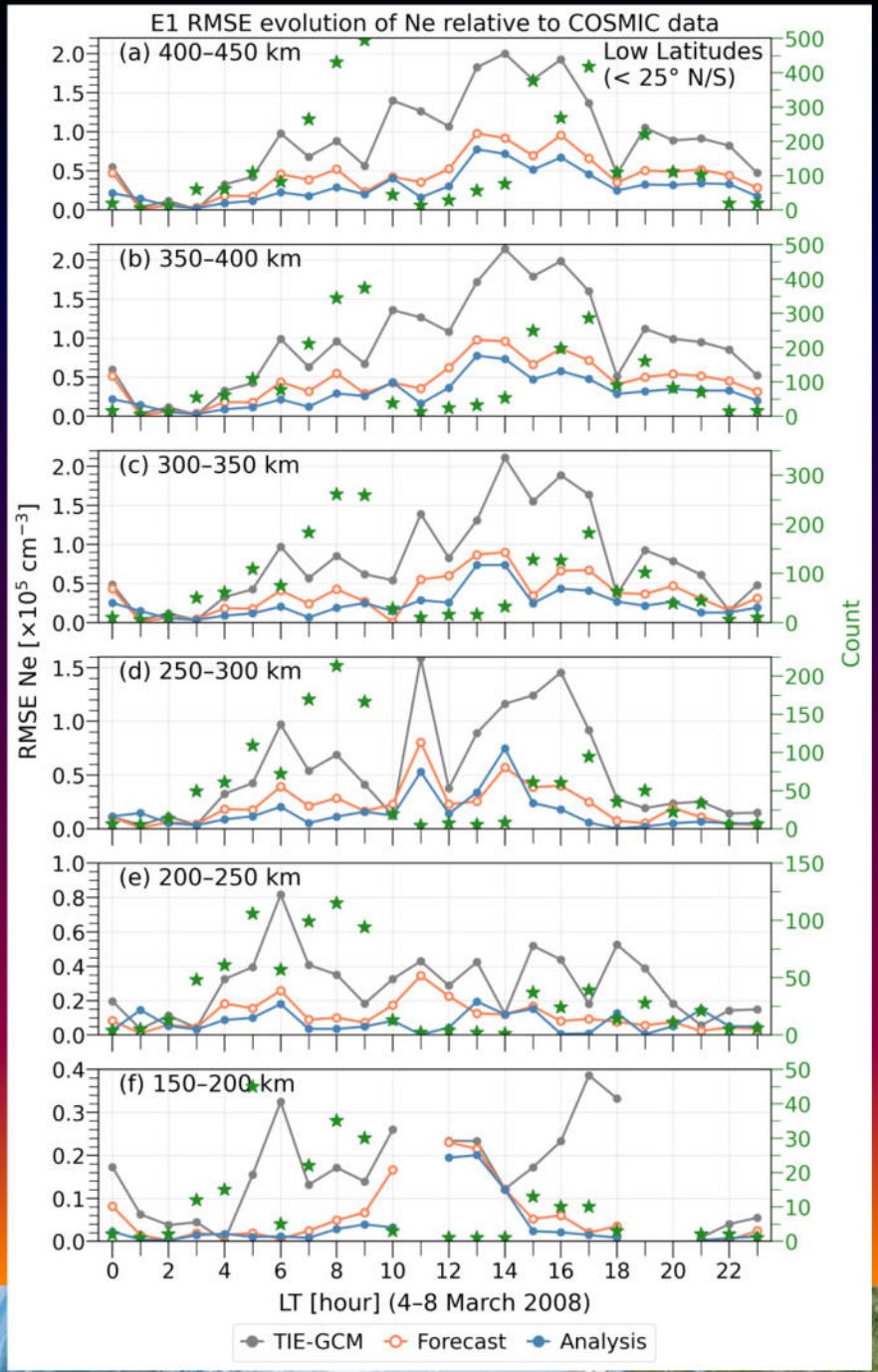
E1 RMSE evolution of Ne relative to COSMIC data
(a) 400–450 km
Low Latitudes
(< 25° N/S)
(b) 350–400 km
(c) 300–350 km
(d) 250–300 km
(e) 200–250 km
(f) 150–200 km
RMSE Ne [×10^5 cm^-3]
Count
LT [hour] (4–8 March 2008)
TIE-GCM
Forecast
Analysis

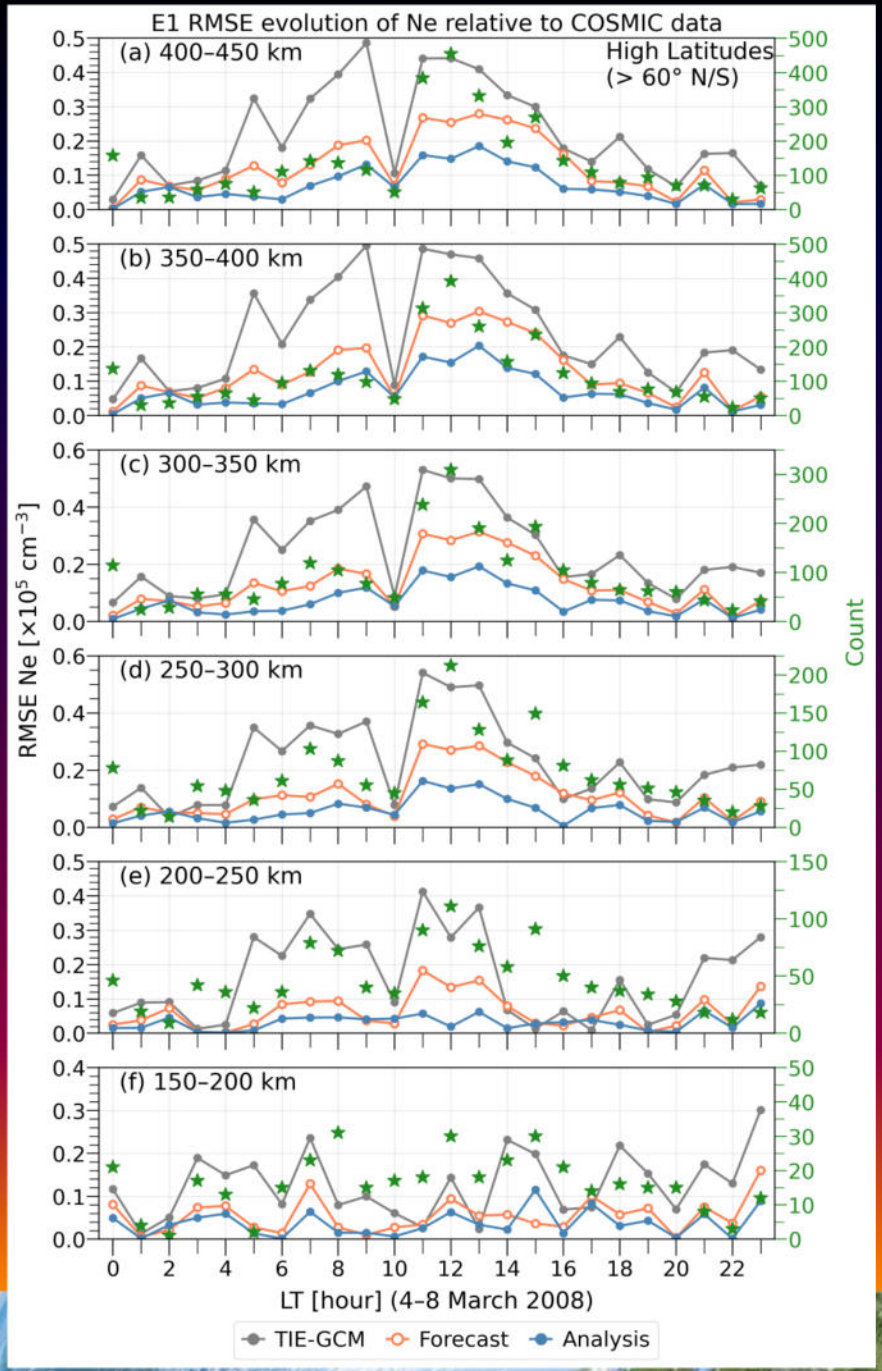
E1 RMSE evolution of Ne relative to COSMIC data
(a) 400–450 km
High Latitudes
(> 60° N/S)
(b) 350–400 km
(c) 300–350 km
(d) 250–300 km
(e) 200–250 km
(f) 150–200 km
RMSE Ne [×10^5 cm^-3]
Count
LT [hour] (4–8 March 2008)
TIE-GCM
Forecast
Analysis

The following three figures are similar to the previous three figures except for E2.

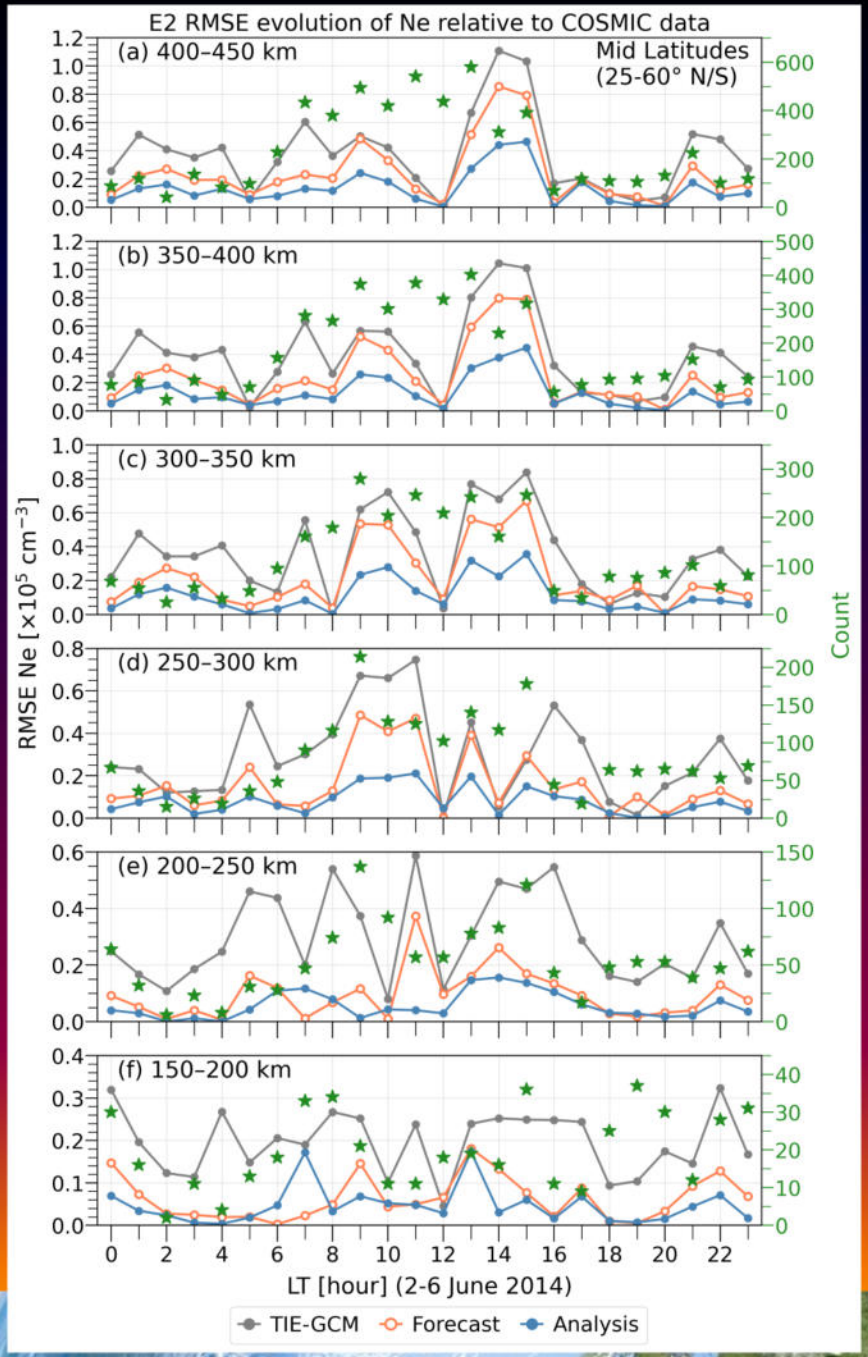
E2 RMSE evolution of Ne relative to COSMIC data
(a) 400–450 km
Mid Latitudes
(25-60° N/S)
(b) 350–400 km
(c) 300–350 km
(d) 250–300 km
(e) 200–250 km
(f) 150–200 km
RMSE Ne [×10^5 cm^-3]
Count
LT [hour] (2-6 June 2014)
TIE-GCM
Forecast
Analysis

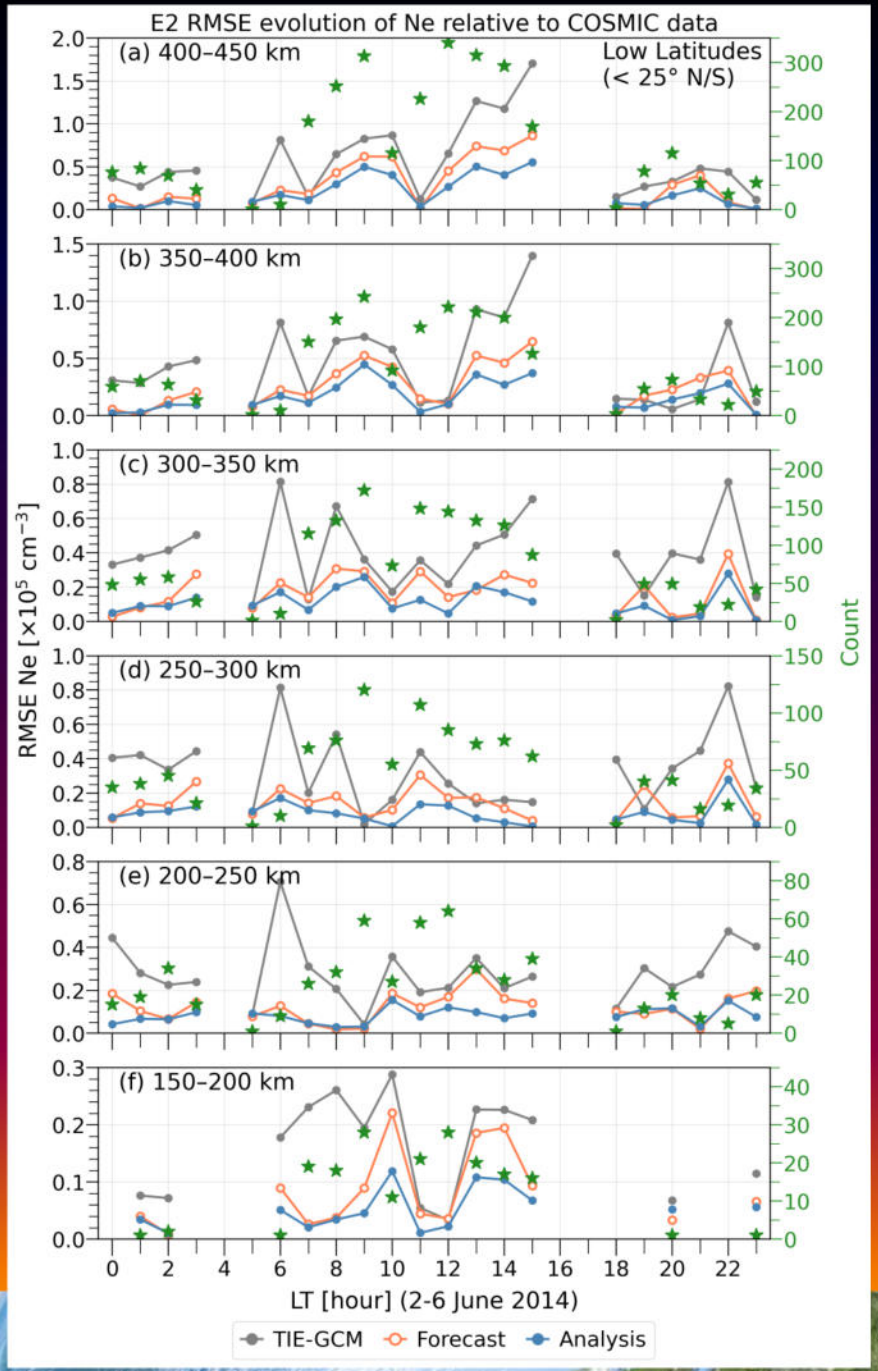
E2 RMSE evolution of Ne relative to COSMIC data
(a) 400–450 km
Low Latitudes
(< 25° N/S)
(b) 350–400 km
(c) 300–350 km
(d) 250–300 km
(e) 200–250 km
(f) 150–200 km
RMSE Ne [×10^5 cm^-3]
Count
LT [hour] (2-6 June 2014)
TIE-GCM
Forecast
Analysis

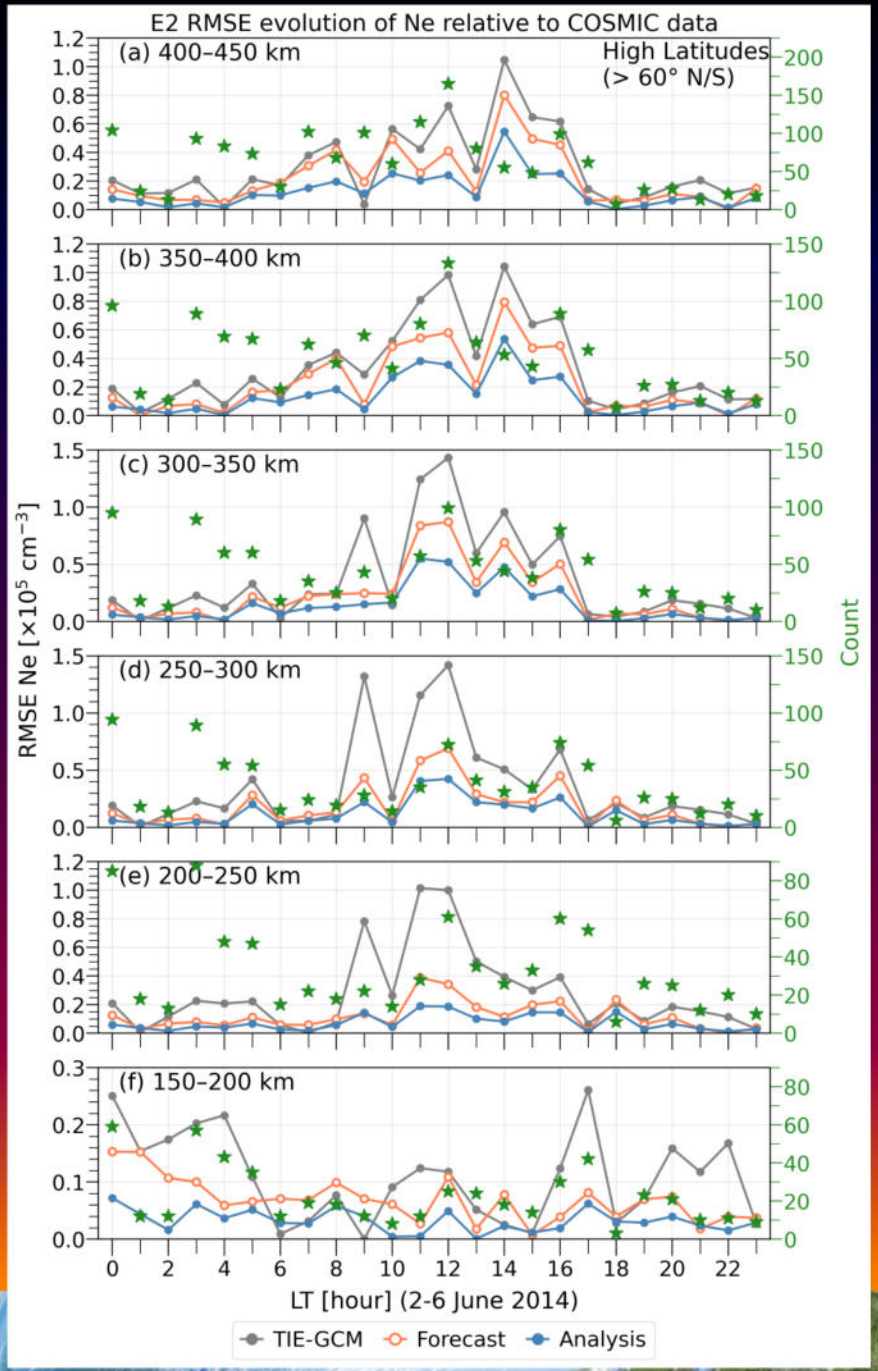
E2 RMSE evolution of Ne relative to COSMIC data
(a) 400–450 km
High Latitudes
(> 60° N/S)
(b) 350–400 km
(c) 300–350 km
(d) 250–300 km
(e) 200–250 km
(f) 150–200 km
RMSE Ne [×10^5 cm^-3]
Count
LT [hour] (2-6 June 2014)
TIE-GCM
Forecast
Analysis

Description of the next figure:

The following figure show an example of the impact of assimilation on the forecasted electron density distribution compared to the 'normal' TIE-GCM run. These are multidimensional scatter plots revealing additional aspects of the compared electron density distributions.

The data points in **orange** indicate whether the particular COSMIC-*Ne* observation was assimilated in the next time step to produce the analysis state. In other words, the forecast shown here is an estimate of the electron density at the observation location with a lead time of one hour. The COSMIC observations that were discarded by the assimilation scheme in the update/analysis step are shown in **gray**. The forecast shown here is only influenced by COSMIC-*Ne* observations that were assimilated in previous time steps and not the particular observation that it is compared to in the current time step. The total number of rejected (assimilated) epochs in the distribution are noted as R (A) in each scatter plot.

Pr = Pearson's correlation coefficient between distributions specified in the abscissa and ordinate.

$\sigma C, \sigma T,$ and σF give the standard deviations (in units of 10^5 cm^{-3}) of COSMIC, TIE-GCM, and forecast, respectively considering the entire population in the specified altitude region.

The solid **blue** line is a least squares polynomial fit of degree 1 considering all epochs, and the black dotted line represents the ideal data-model reference.

Figure also indicates the geographic latitude of the epochs in three categories: **low** (25° S-25° N; triangle), **middle** (25°-60° N/S; cross), and **high** (60°-90° N/S; dot).

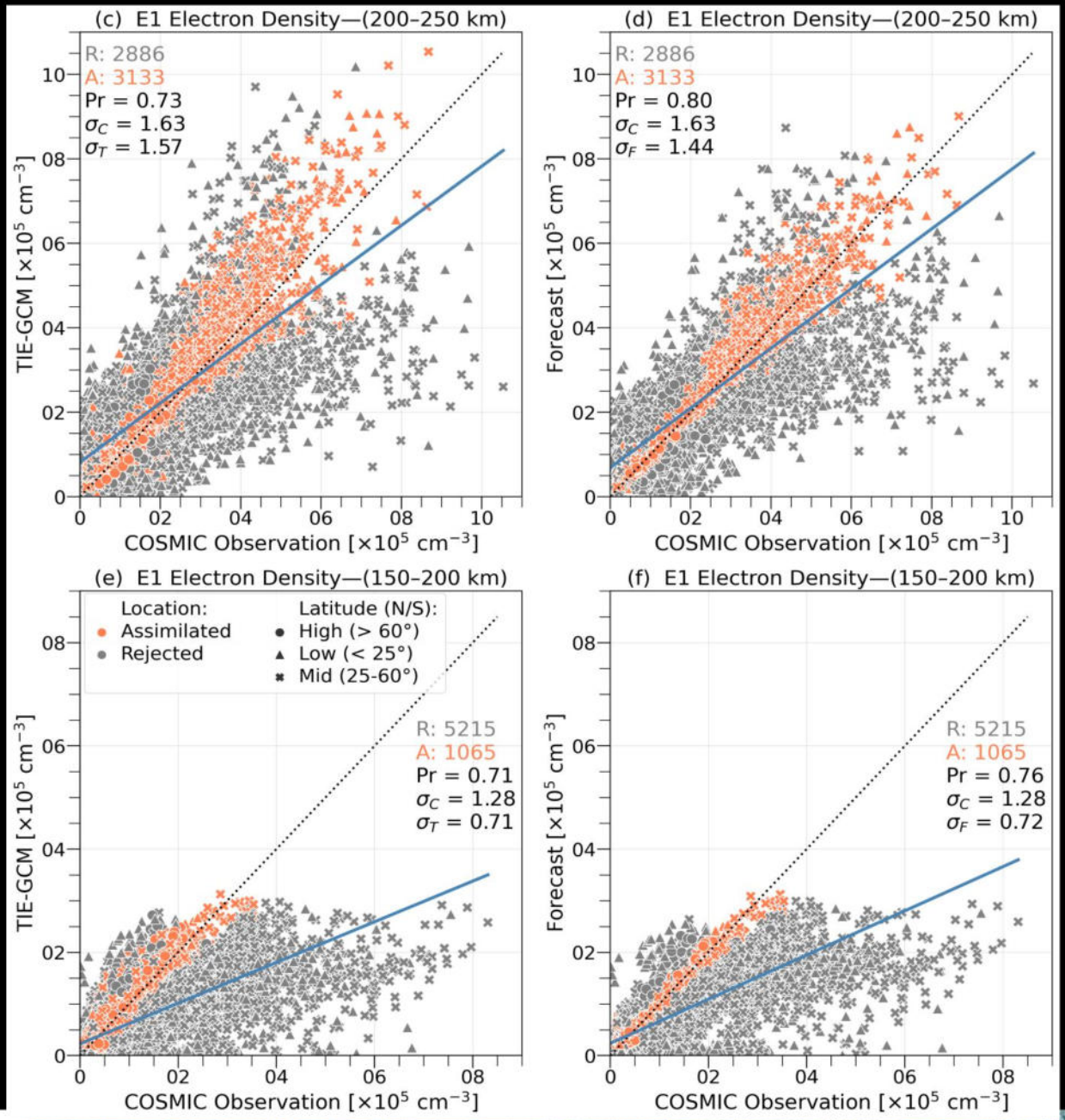

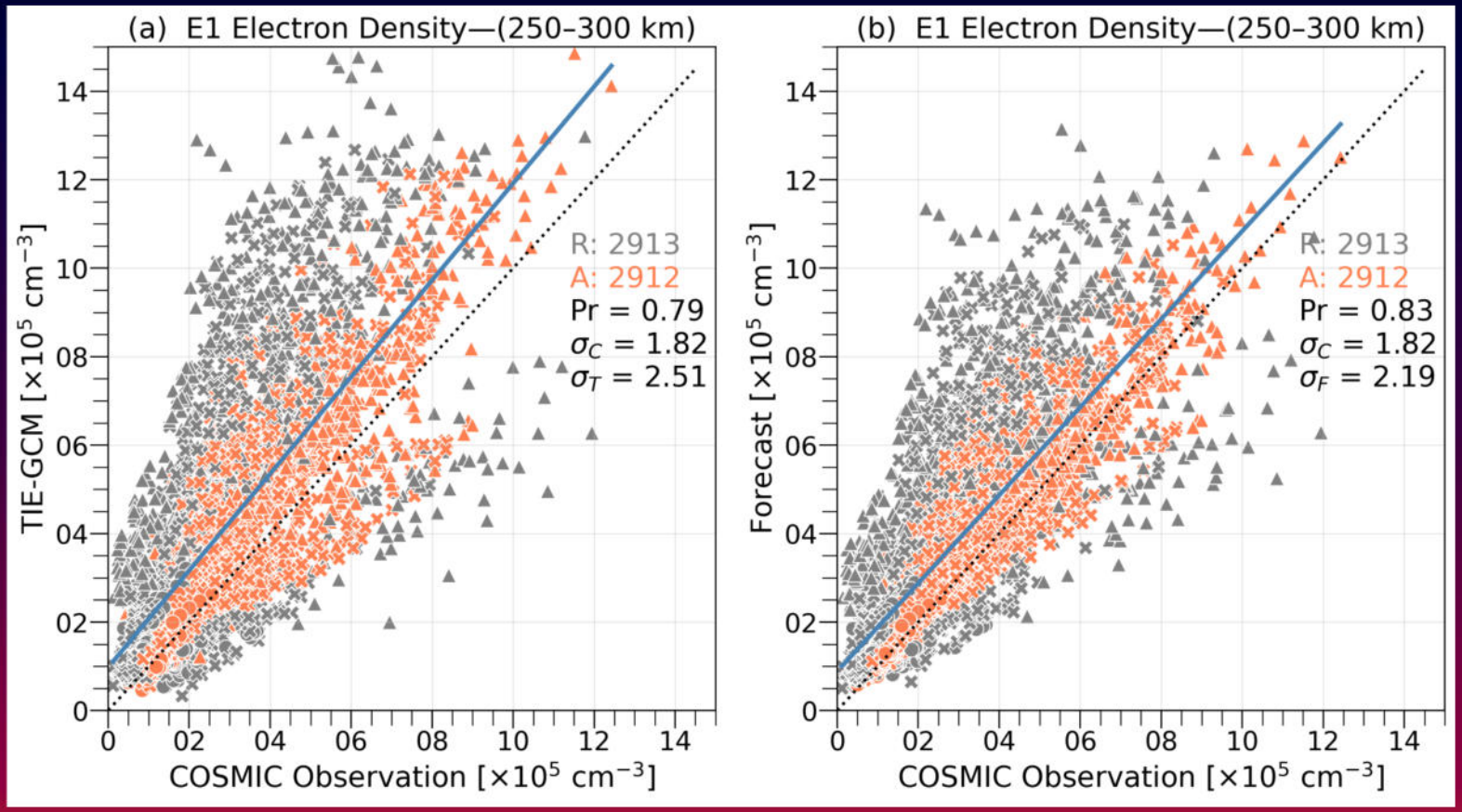
(a) E1 Electron Density—(250–300 km)
TIE-GCM [×10^5 cm^−3]
COSMIC Observation [×10^5 cm^−3]
R: 2913
A: 2912
Pr = 0.79
σ_C = 1.82
σ_T = 2.51
(b) E1 Electron Density—(250–300 km)
Forecast [×10^5 cm^−3]
COSMIC Observation [×10^5 cm^−3]
R: 2913
A: 2912
Pr = 0.83
σ_C = 1.82
σ_F = 2.19

Same as above except for E2.

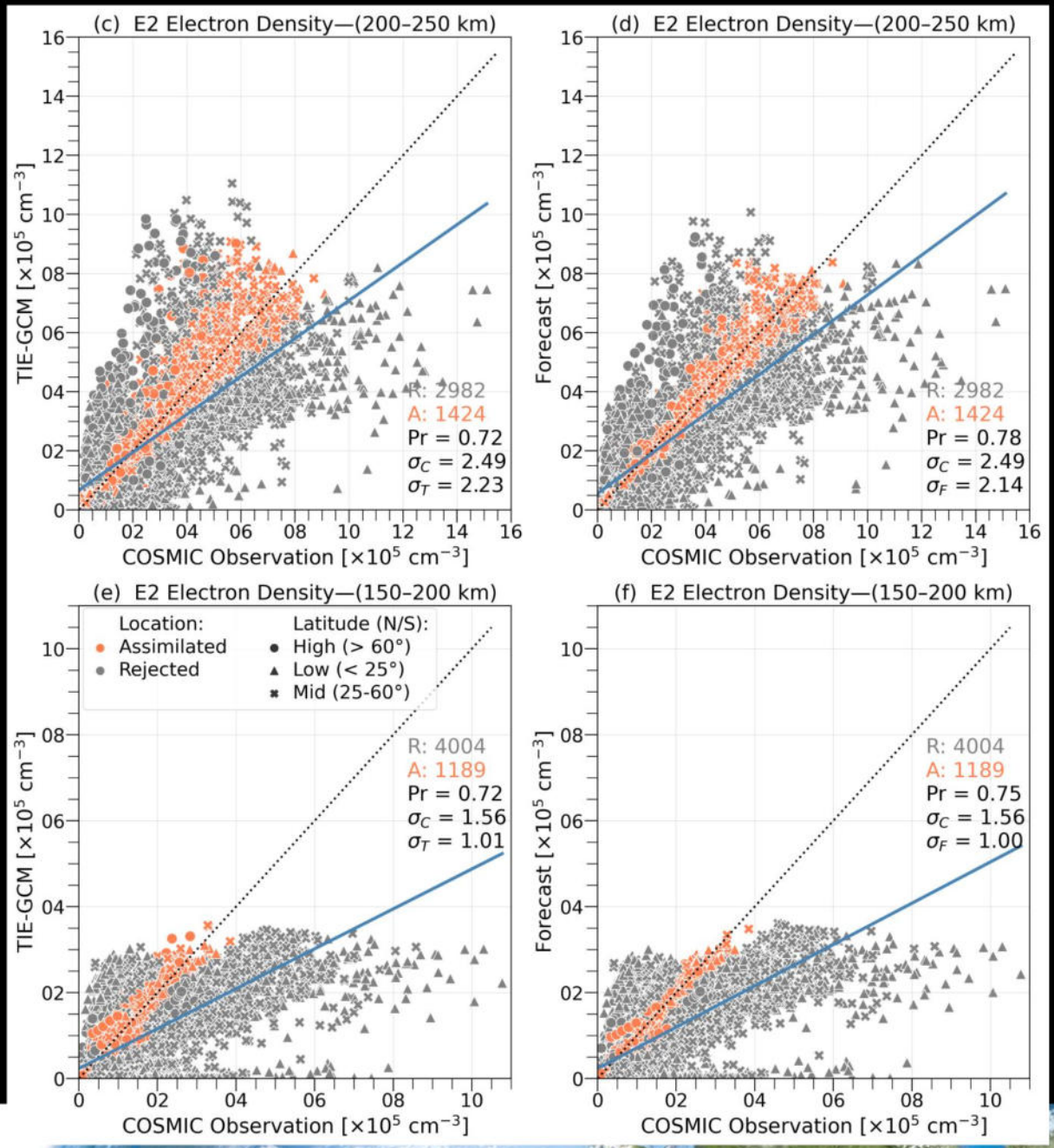

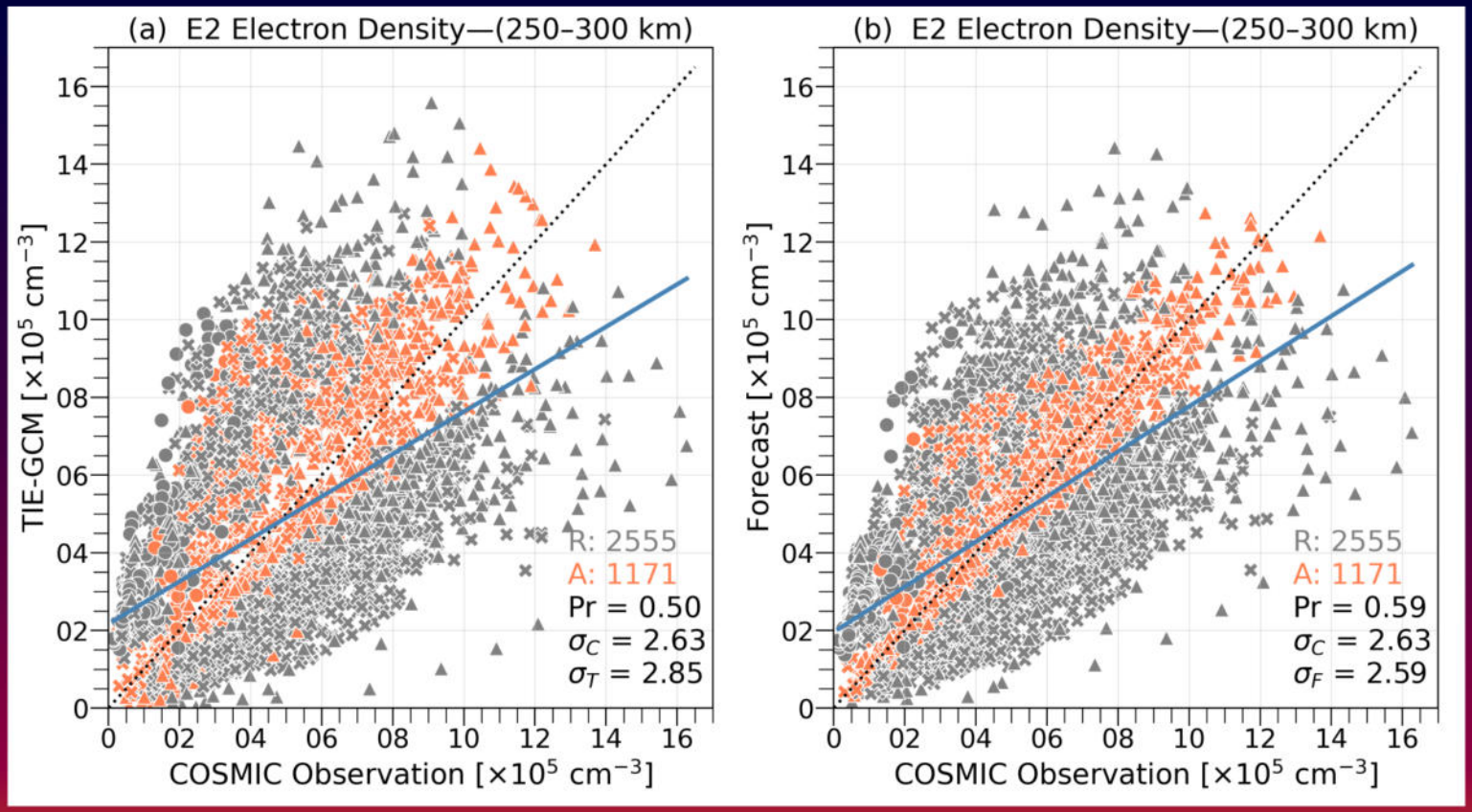
(a) E2 Electron Density—(250–300 km)
TIE-GCM [×10^5 cm^−3]
COSMIC Observation [×10^5 cm^−3]
R: 2555
A: 1171
Pr = 0.50
σC = 2.63
σT = 2.85
(b) E2 Electron Density—(250–300 km)
Forecast [×10^5 cm^−3]
COSMIC Observation [×10^5 cm^−3]
R: 2555
A: 1171
Pr = 0.59
σC = 2.63
σF = 2.59

The following figure summarizes the assimilation results of both E1 and E2 relative to COSMIC observations.

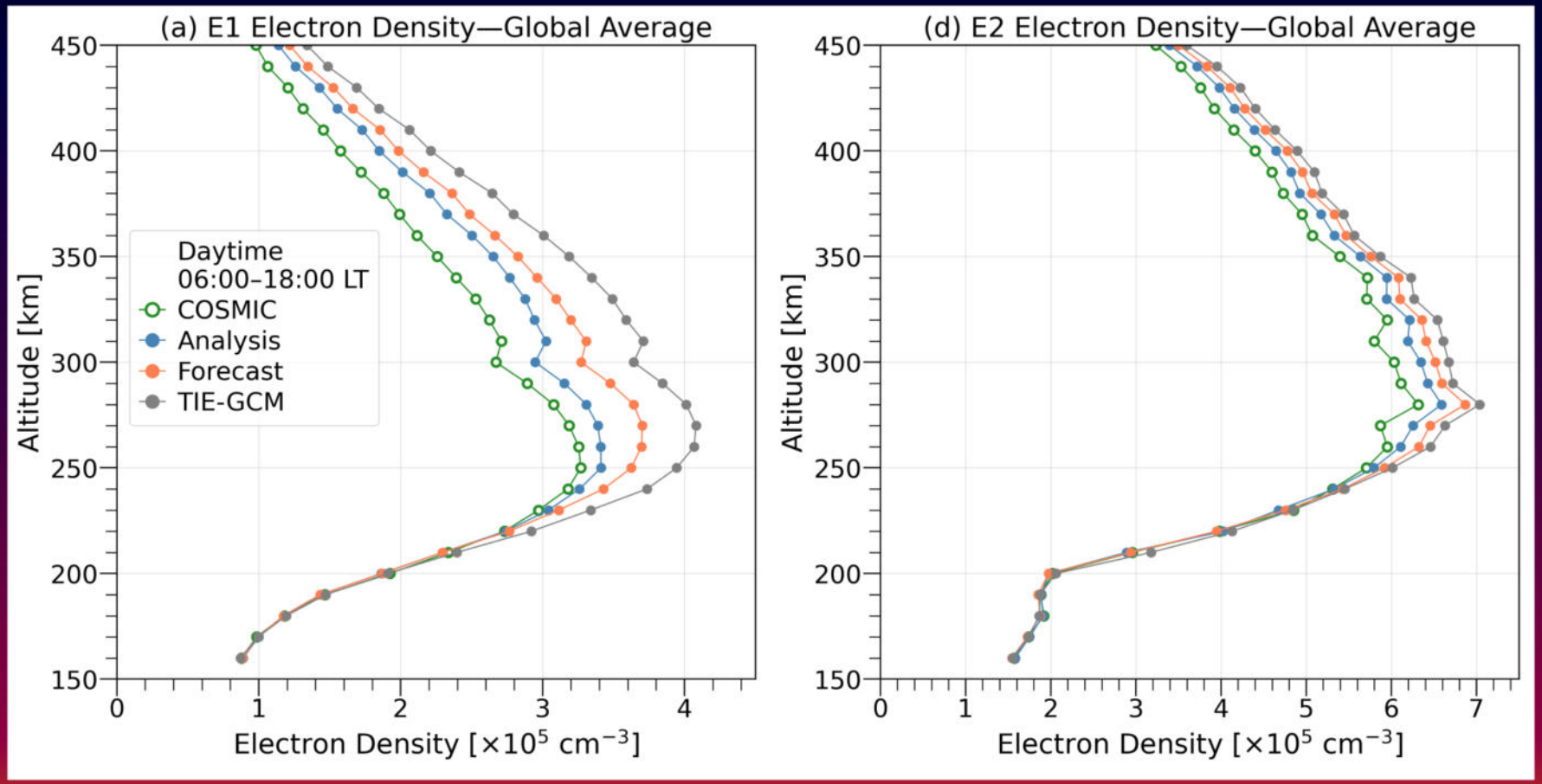
(a) E1 Electron Density—Global Average
(d) E2 Electron Density—Global Average
Altitude [km]
Electron Density [×10^5 cm^−3]
Daytime
06:00–18:00 LT
COSMIC
Analysis
Forecast
TIE-GCM

Daytime

$\sigma C, \sigma T, , \sigma A,$ and σF give the standard deviations (in units of 10^5 cm^{-3}) of COSMIC, TIE-GCM, analysis, and forecast, respectively considering the entire population in the specified altitude region.

The solid black line is a least squares polynomial fit of degree 1 considering all epochs, and the black dotted line represents the ideal data-model reference.

Here the data are binned by the resolution of the input COSMIC data (i.e. 10 km).

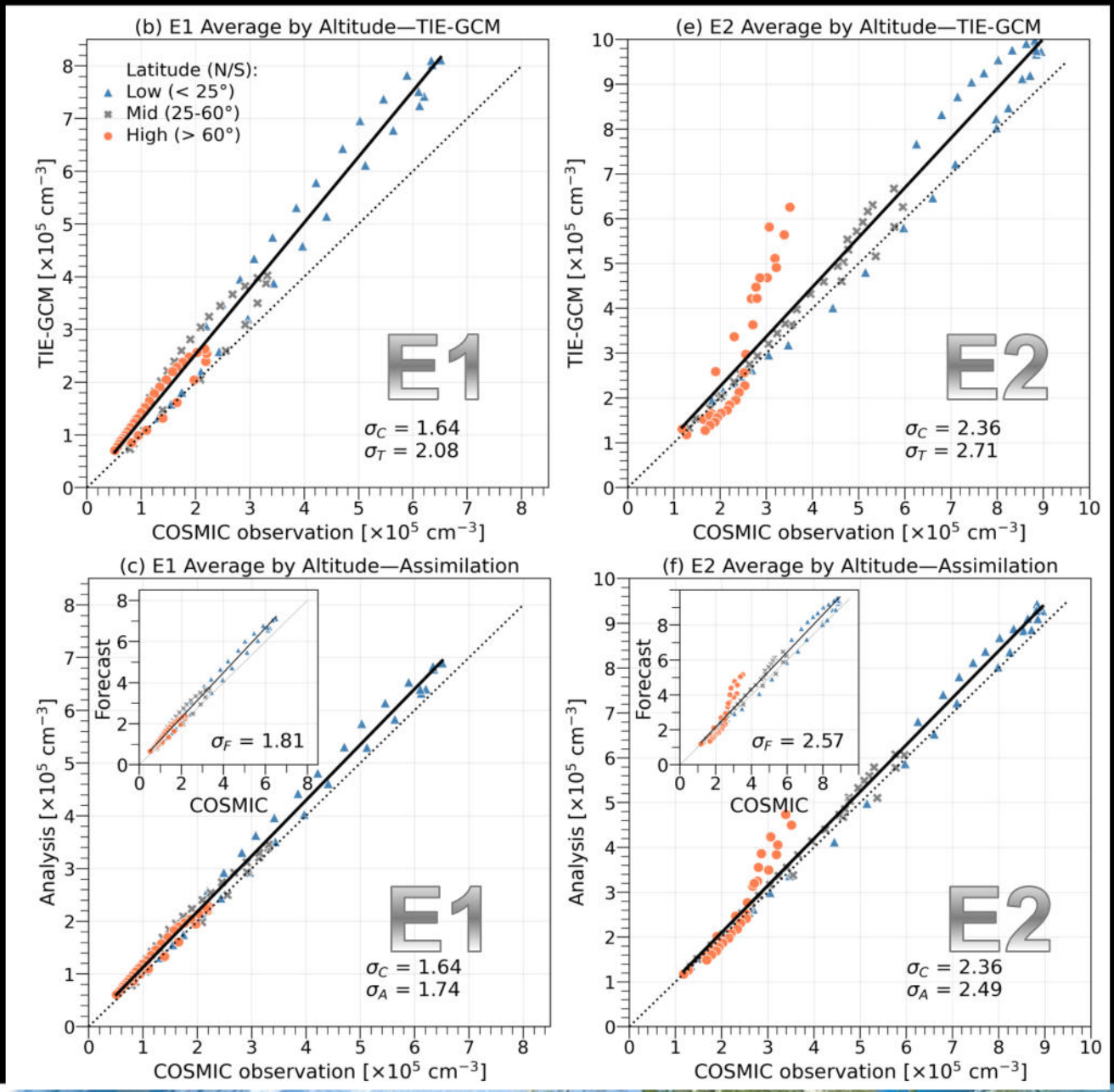

The following figure is similar to the previous figure except for night-time electron density profile.

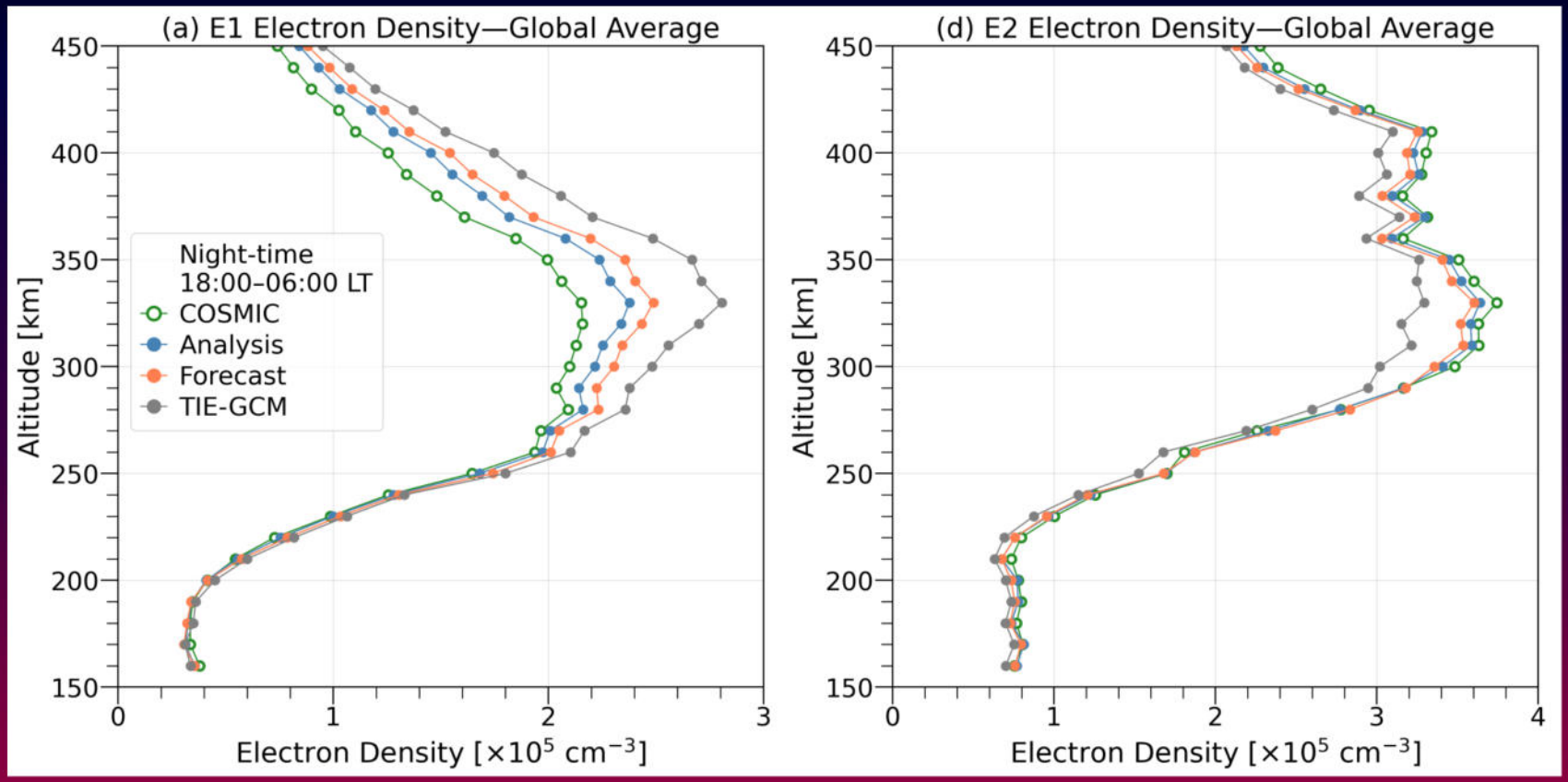
(a) E1 Electron Density—Global Average
(d) E2 Electron Density—Global Average
Night-time
18:00–06:00 LT
COSMIC
Analysis
Forecast
TIE-GCM
Altitude [km]
Electron Density [×10^5 cm^−3]
450
400
350
300
250
200
150
0
1
2
3
4

Night-time

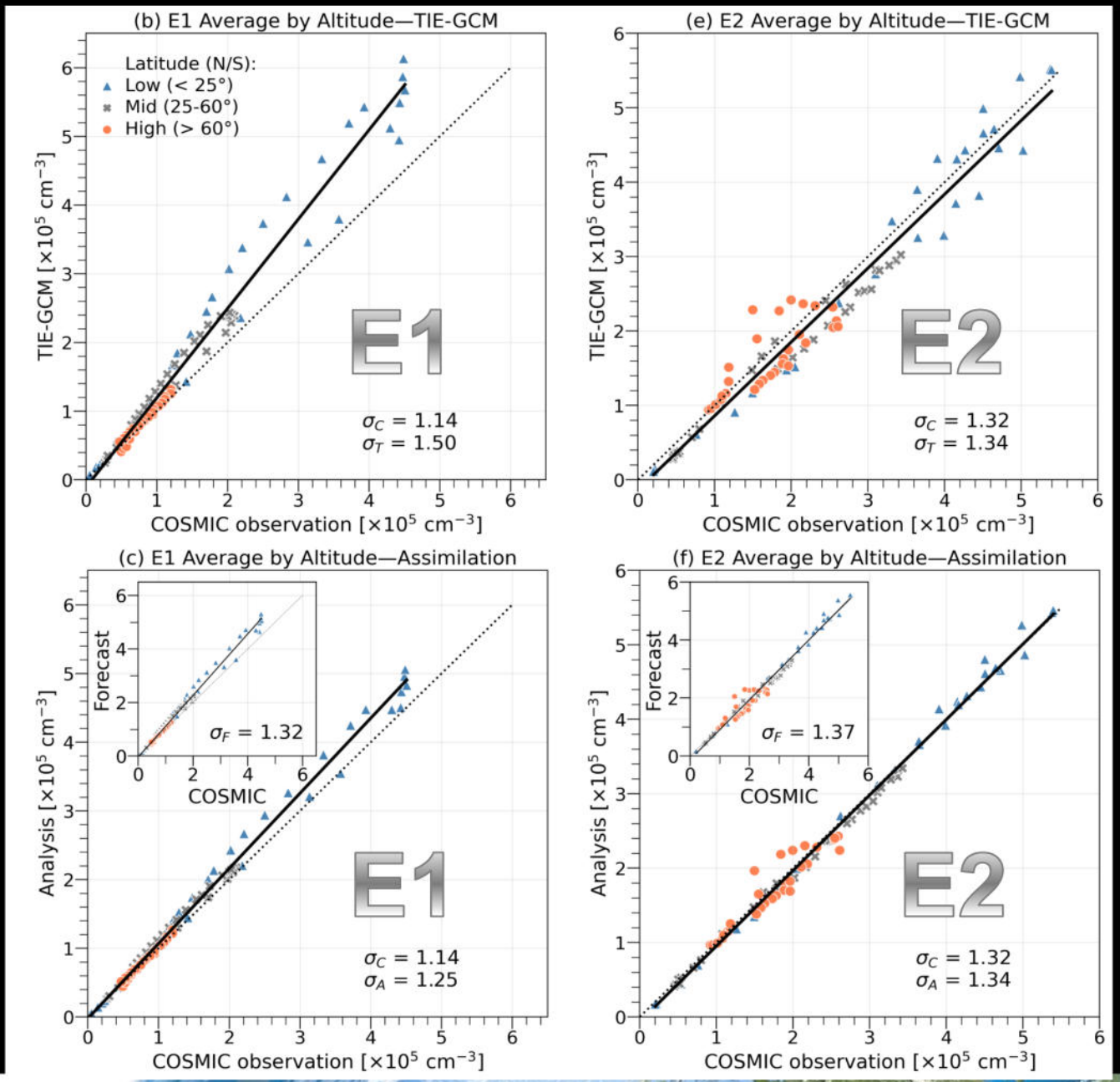
(b) E1 Average by Altitude—TIE-GCM
Latitude (N/S):
Low (< 25°)
Mid (25-60°)
High (> 60°)
TIE-GCM [×10^5 cm^−3]
COSMIC observation [×10^5 cm^−3]
E1
σC = 1.14
σT = 1.50
(e) E2 Average by Altitude—TIE-GCM
TIE-GCM [×10^5 cm^−3]
COSMIC observation [×10^5 cm^−3]
E2
σC = 1.32
σT = 1.34
(c) E1 Average by Altitude—Assimilation
Forecast
COSMIC
σF = 1.32
Analysis [×10^5 cm^−3]
COSMIC observation [×10^5 cm^−3]
E1
σC = 1.14
σA = 1.25
(f) E2 Average by Altitude—Assimilation
Forecast
COSMIC
σF = 1.37
Analysis [×10^5 cm^−3]
COSMIC observation [×10^5 cm^−3]
E2
σC = 1.32
σA = 1.34

Validation of Forecasts Against Independent Data

E1

E1 compared to GRACE electron density profile retrieved through RO.

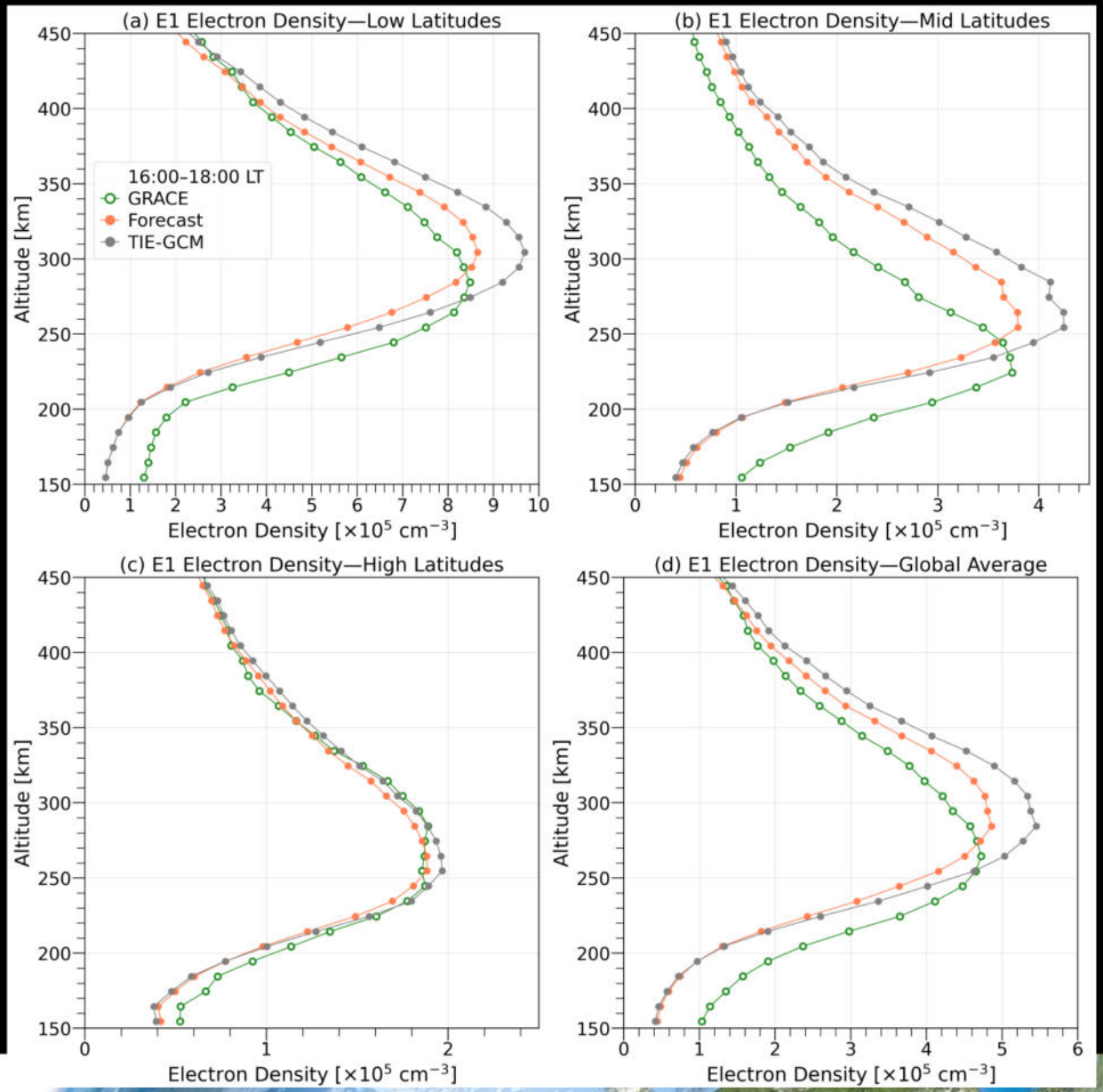

E1

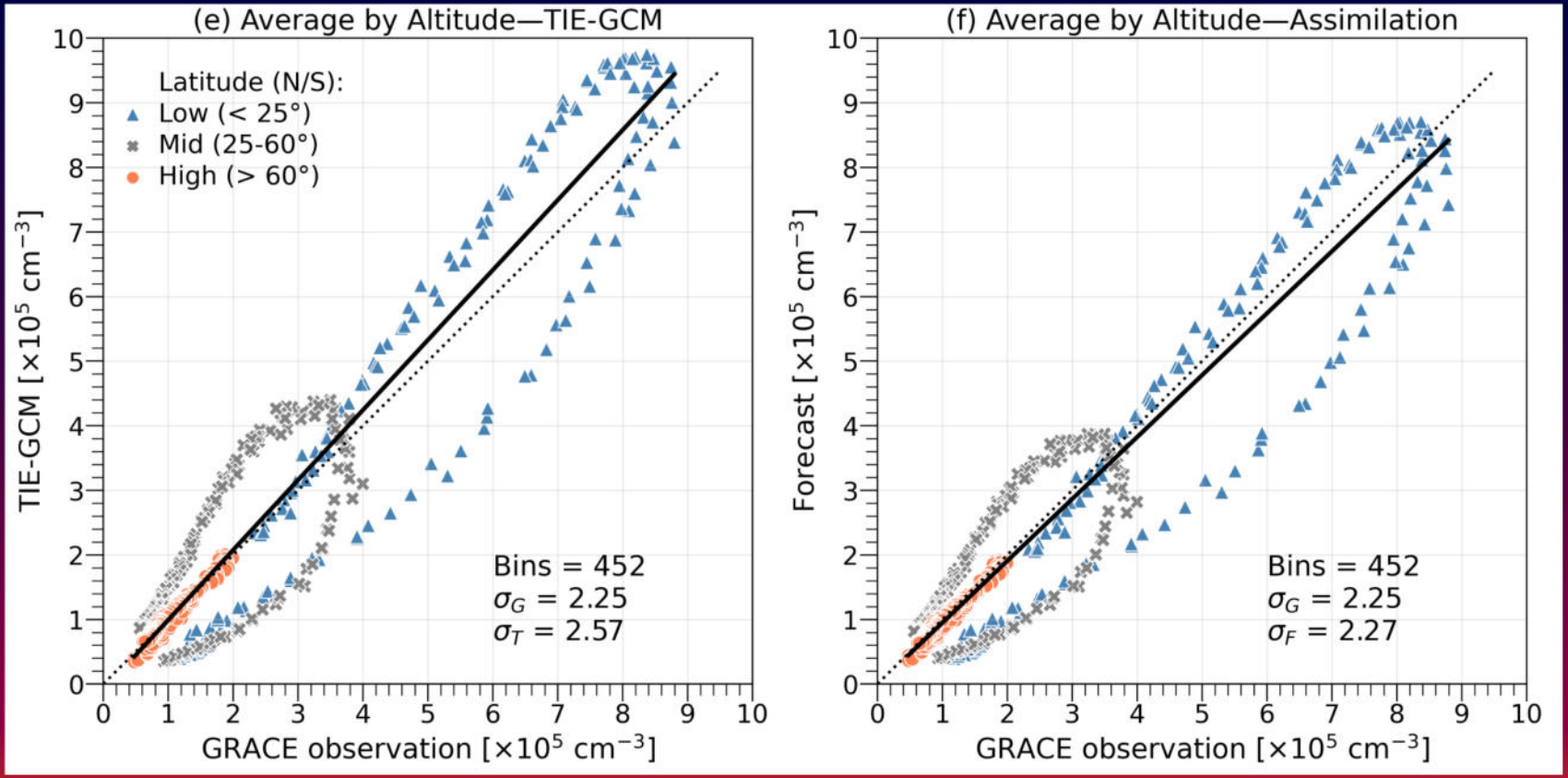
(e) Average by Altitude—TIE-GCM
Latitude (N/S):
Low (< 25°)
Mid (25-60°)
High (> 60°)
Bins = 452
σ_G = 2.25
σ_T = 2.57
TIE-GCM [×10^5 cm^{-3}]
GRACE observation [×10^5 cm^{-3}]
(f) Average by Altitude—Assimilation
Bins = 452
σ_G = 2.25
σ_F = 2.27
Forecast [×10^5 cm^{-3}]
GRACE observation [×10^5 cm^{-3}]

E1

E1 compared to electron density along the CHAMP orbit.

Closeness = where the estimated values from one model are more closer to CHAMP data than the other.

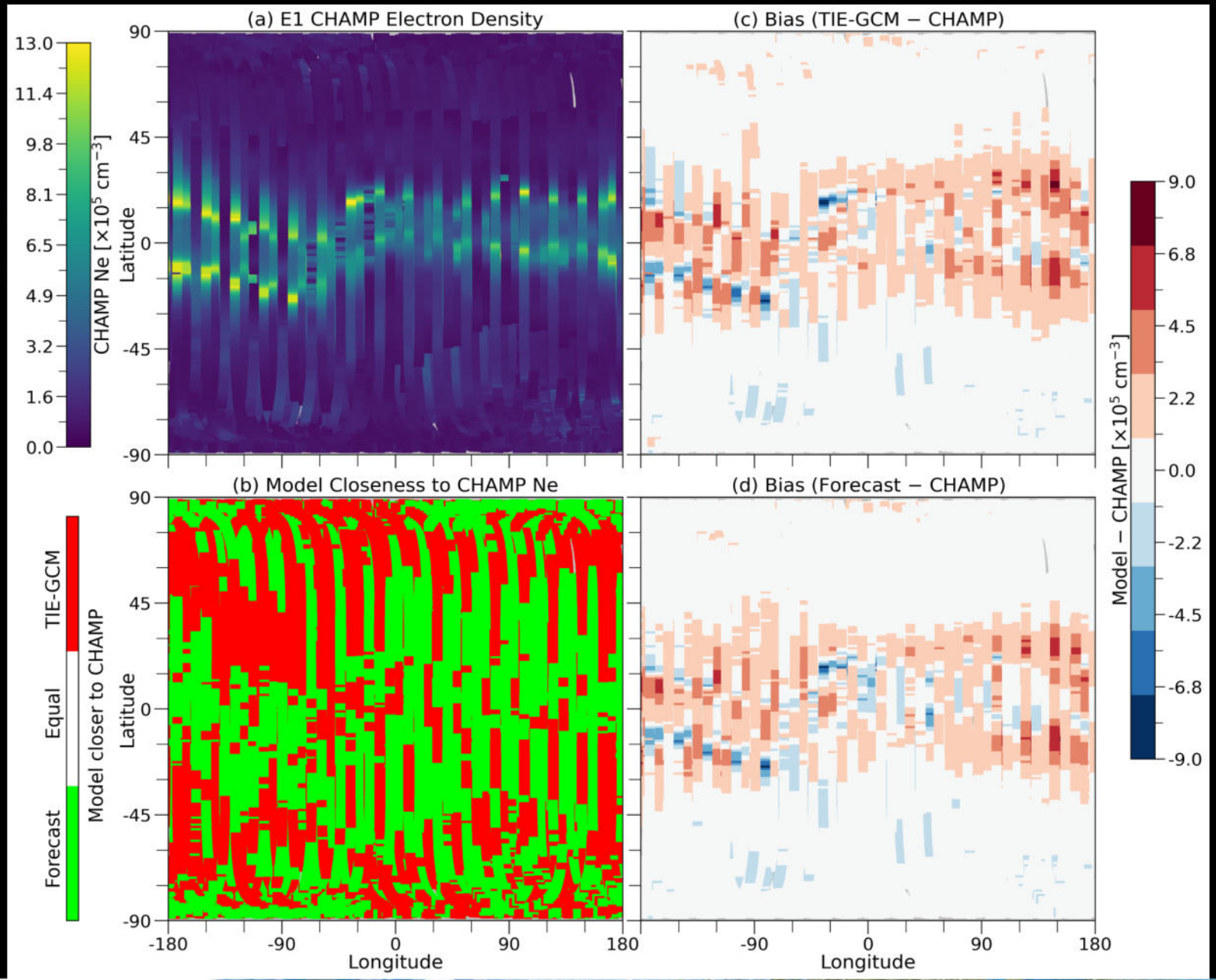

E1

E1 compared to electron density along the CHAMP orbit's descending and ascending segments

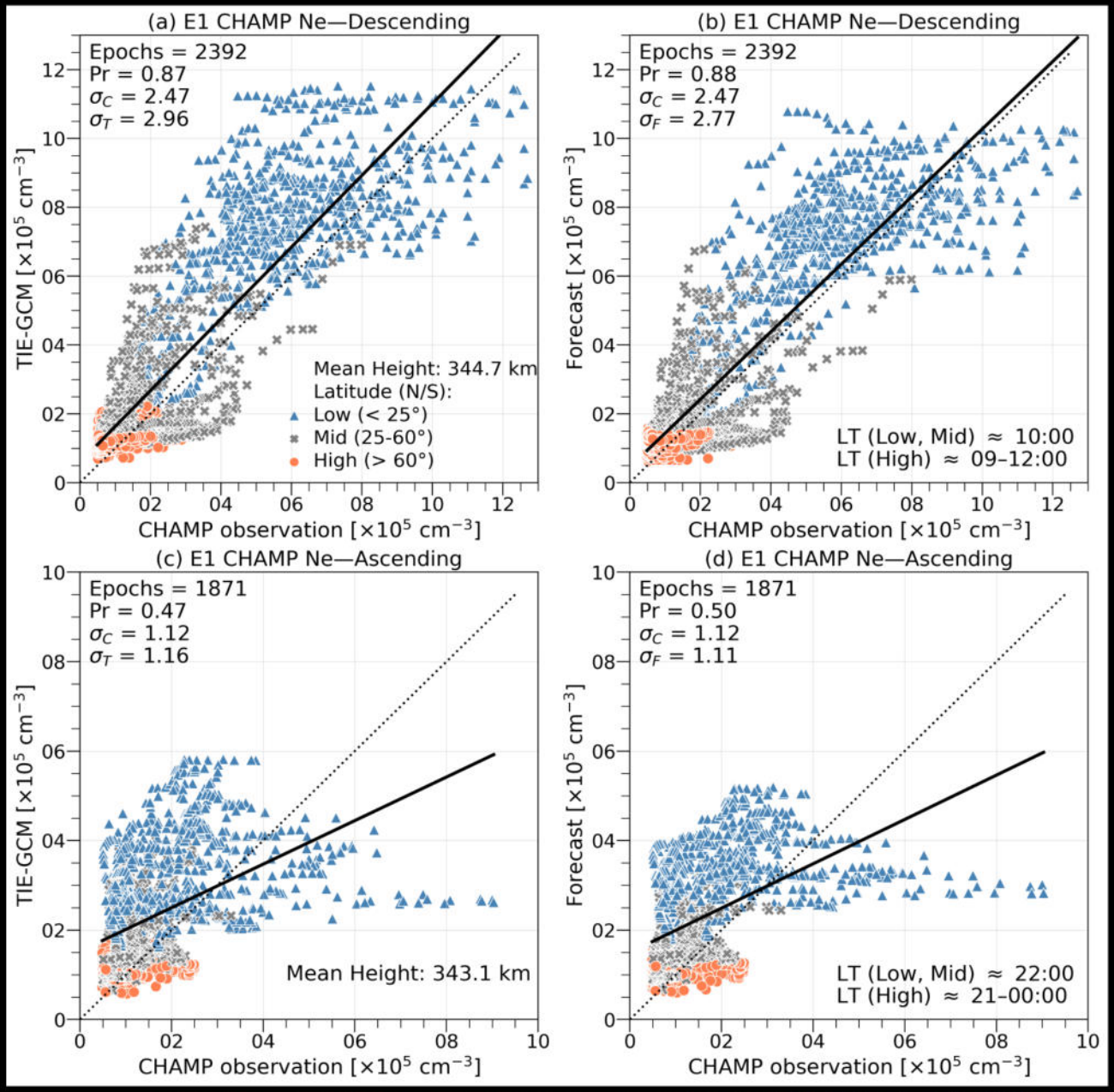

E2

E2 compared to GRACE electron density profile retrieved through RO.

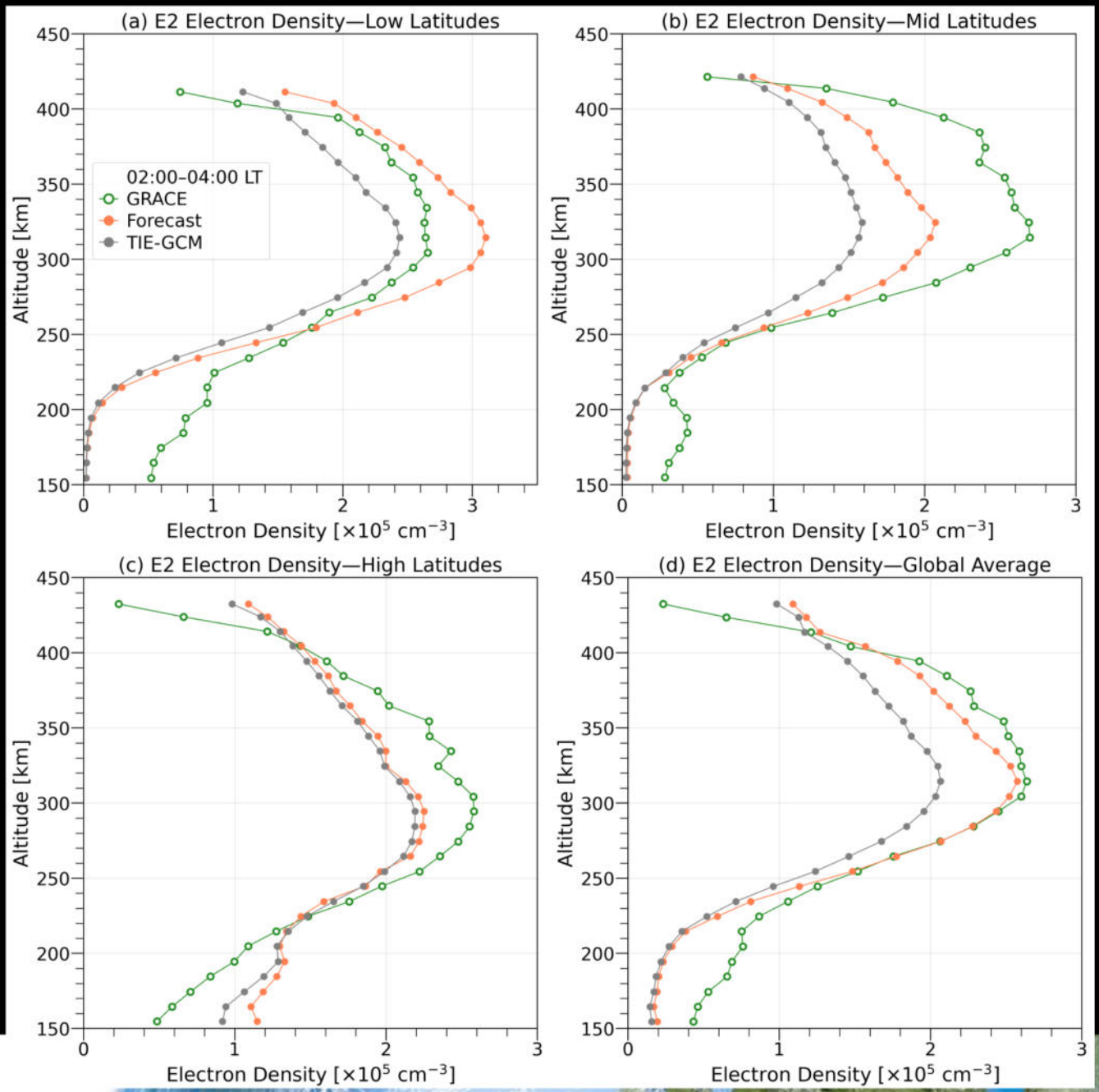

E2

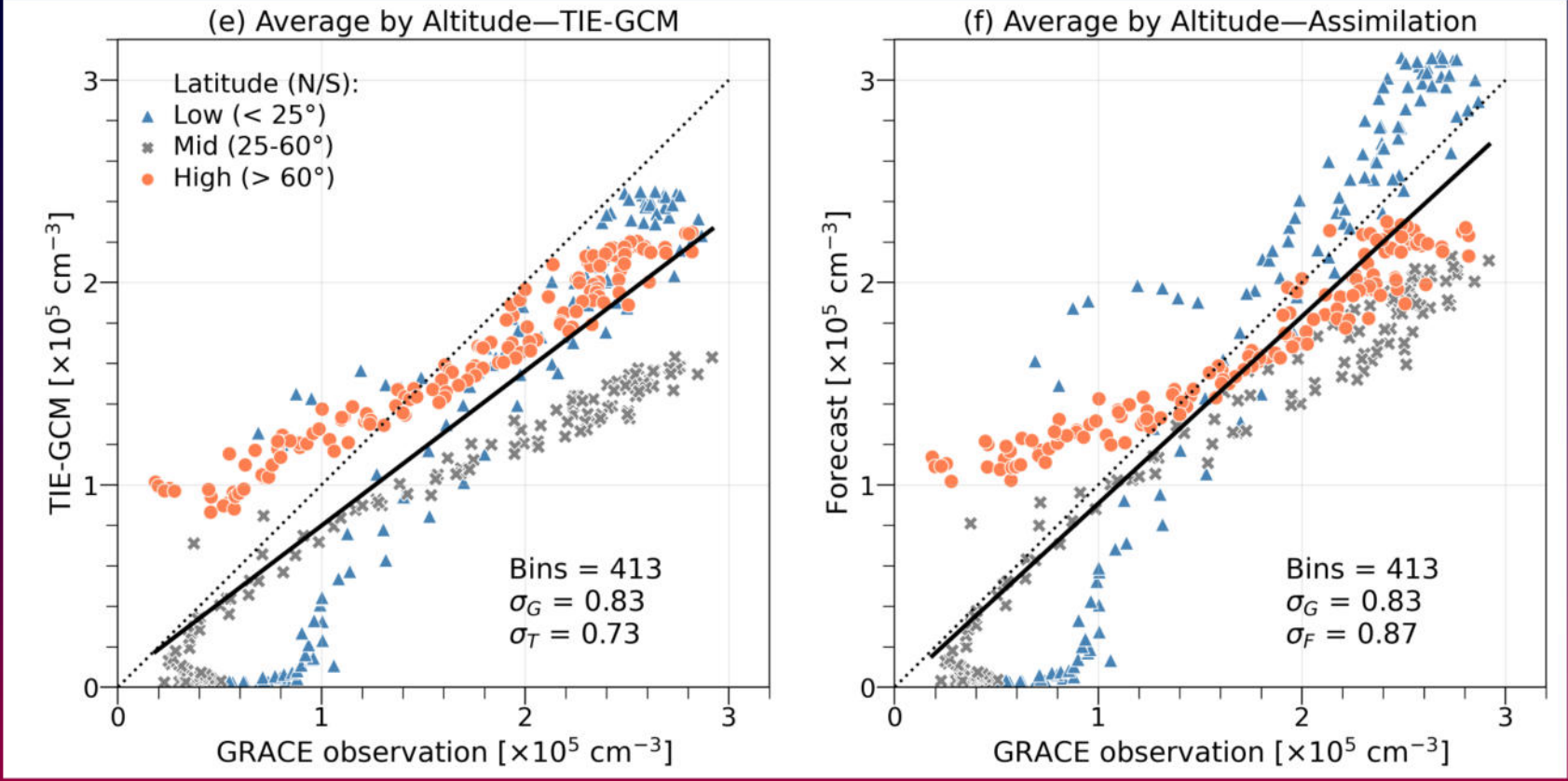
(e) Average by Altitude—TIE-GCM
Latitude (N/S):
Low (< 25°)
Mid (25-60°)
High (> 60°)
TIE-GCM [×10^5 cm^−3]
GRACE observation [×10^5 cm^−3]
Bins = 413
σ_G = 0.83
σ_T = 0.73
(f) Average by Altitude—Assimilation
Forecast [×10^5 cm^−3]
GRACE observation [×10^5 cm^−3]
Bins = 413
σ_G = 0.83
σ_F = 0.87

Impact of the Assimilation on the Thermosphere

The following figures show longitude-latitude maps of neutral mass density (ρ) at a few selected altitude levels and UTs. The left column shows the estimated ρ from TIE-GCM, forecast, and analysis runs. Their differences are shown in the right column. The **cyan** dots indicate the location of COSMIC-*Ne* data that were assimilated since 2.5 hours prior to the time indicated in the snapshot.

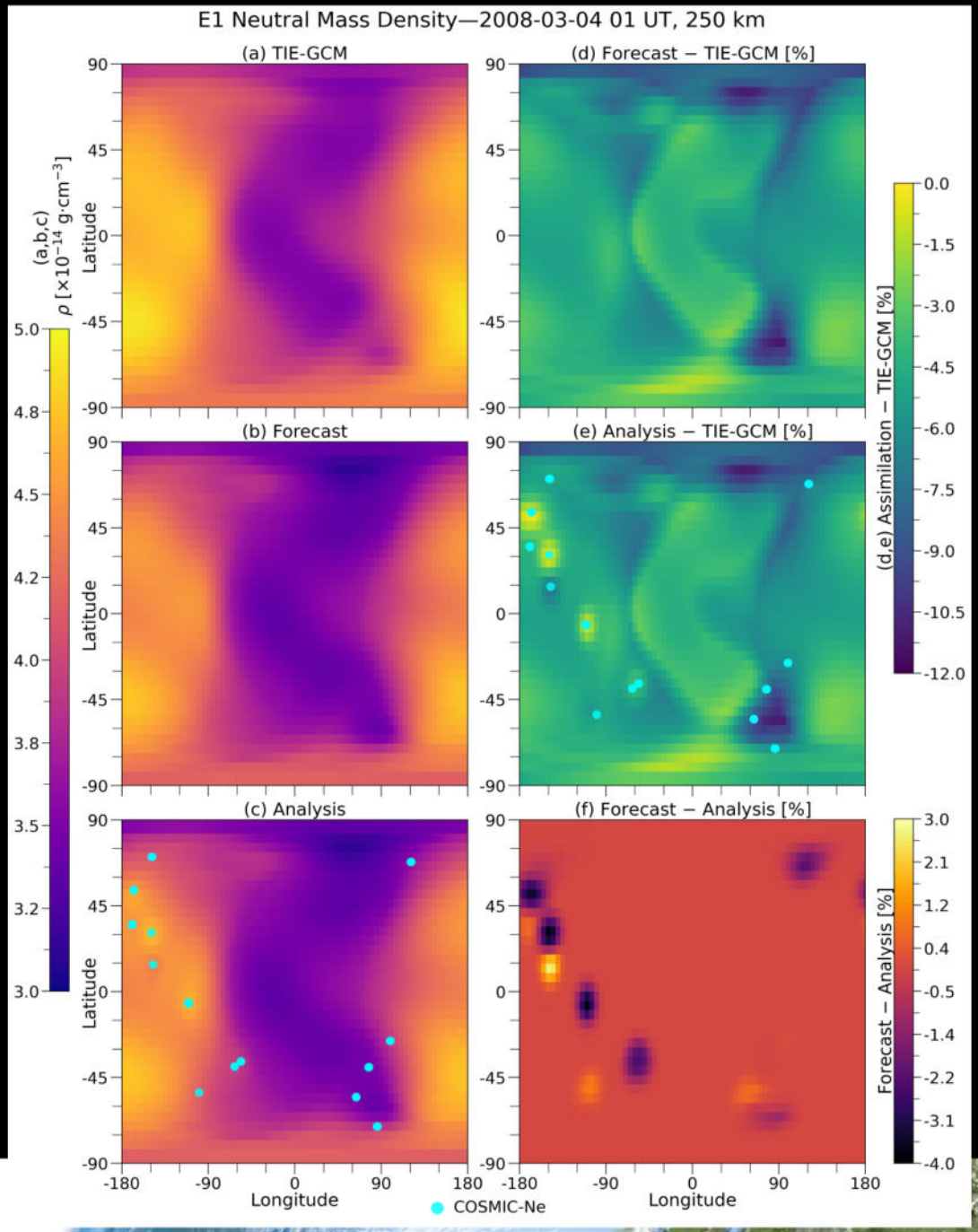
E1 Neutral Mass Density—2008-03-04 01 UT, 250 km
(a) TIE-GCM
(d) Forecast − TIE-GCM [%]
(b) Forecast
(e) Analysis − TIE-GCM [%]
(c) Analysis
(f) Forecast − Analysis [%]
(a,b,c) ρ [×10⁻¹⁴ g·cm⁻³]
(d,e) Assimilation − TIE-GCM [%]
Forecast − Analysis [%]
Latitude
Longitude
COSMIC-Ne

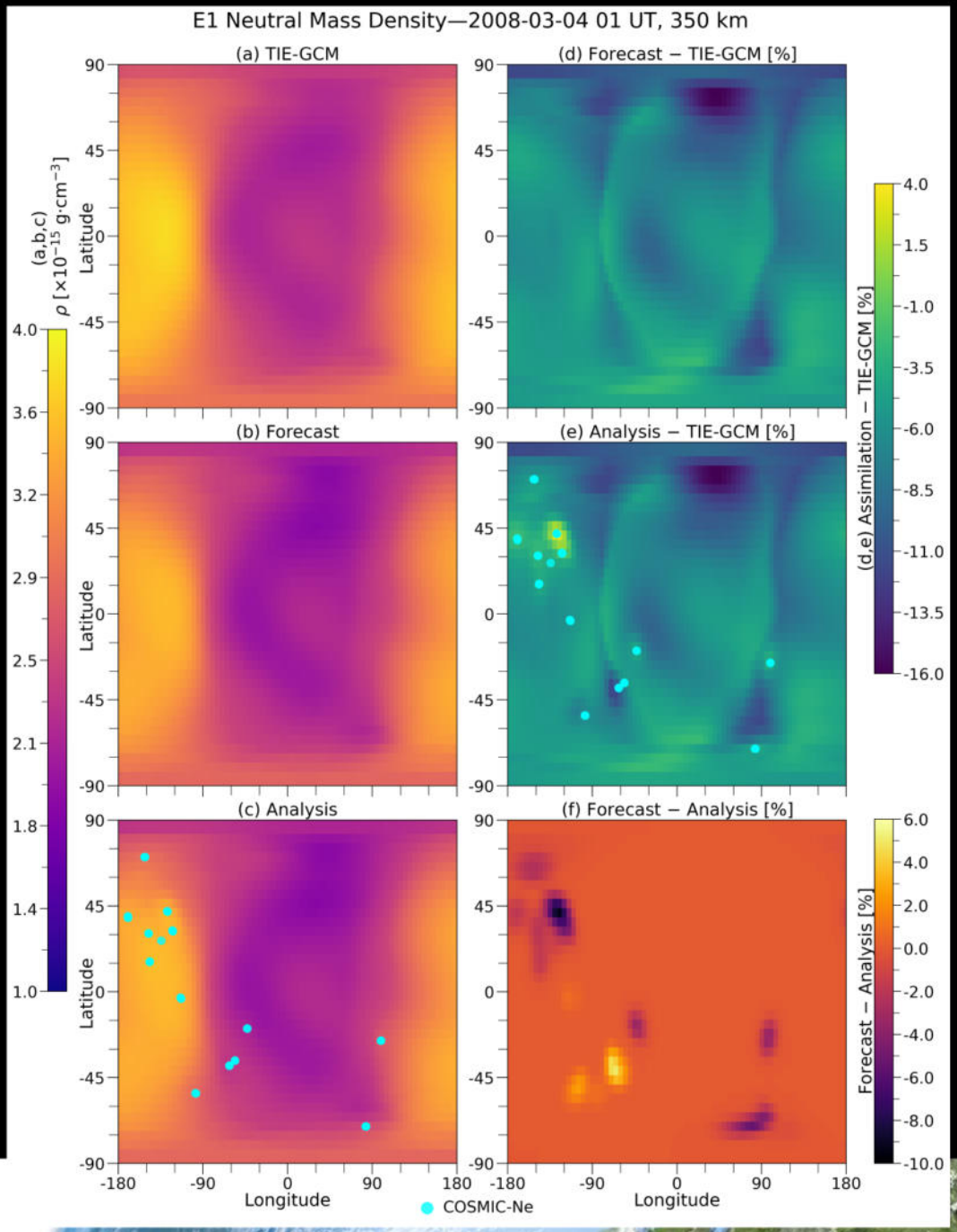
E1 Neutral Mass Density—2008-03-04 01 UT, 350 km
(a) TIE-GCM
(d) Forecast − TIE-GCM [%]
(b) Forecast
(e) Analysis − TIE-GCM [%]
(c) Analysis
(f) Forecast − Analysis [%]
(a,b,c) ρ [×10⁻¹⁵ g·cm⁻³]
(d,e) Assimilation − TIE-GCM [%]
Forecast − Analysis [%]
Latitude
Longitude
COSMIC-Ne

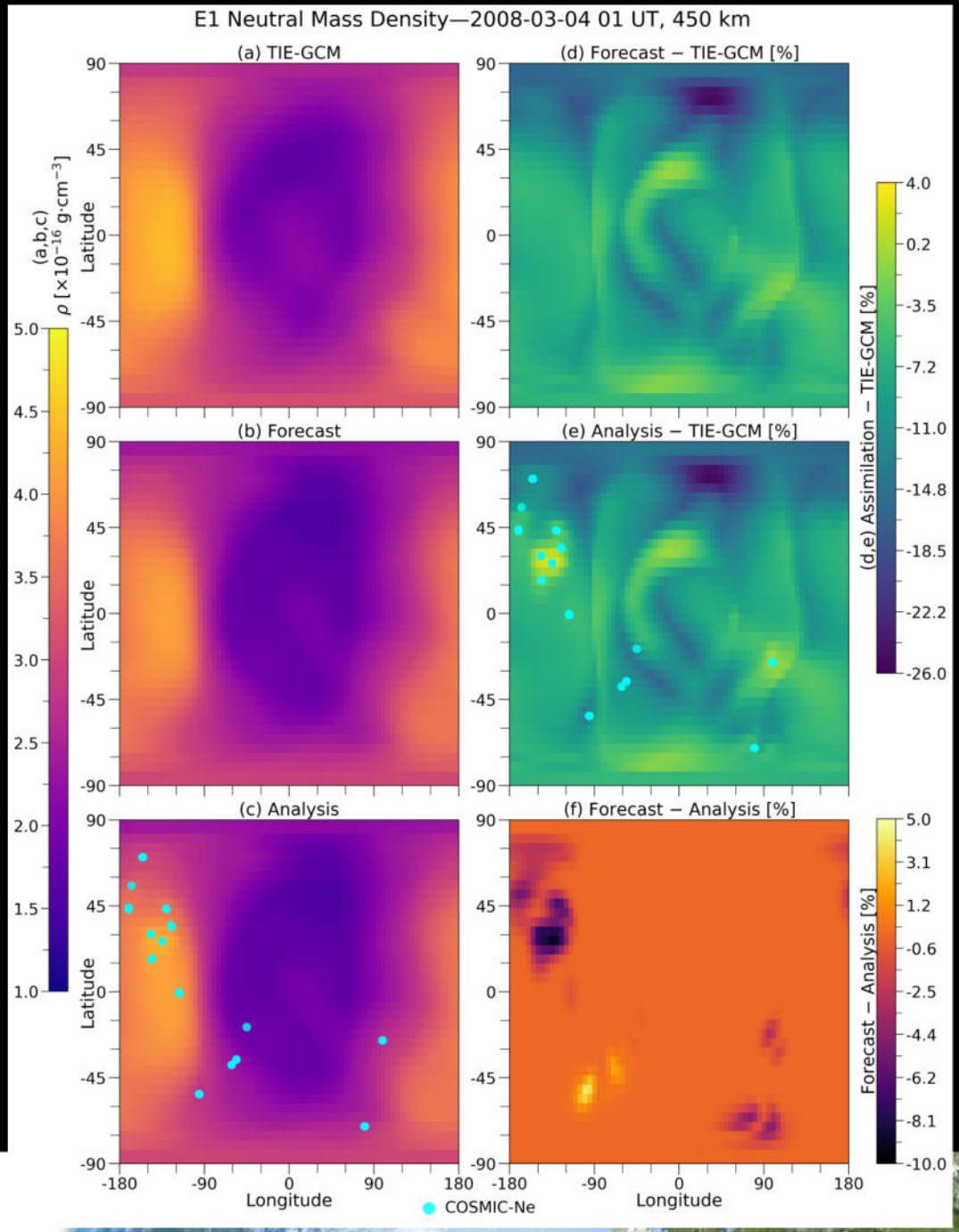
E1 Neutral Mass Density—2008-03-04 01 UT, 450 km
(a) TIE-GCM
(d) Forecast − TIE-GCM [%]
(b) Forecast
(e) Analysis − TIE-GCM [%]
(c) Analysis
(f) Forecast − Analysis [%]
(a,b,c) ρ [×10⁻¹⁶ g·cm⁻³]
(d,e) Assimilation − TIE-GCM [%]
Forecast − Analysis [%]
Latitude
Longitude
COSMIC-Ne

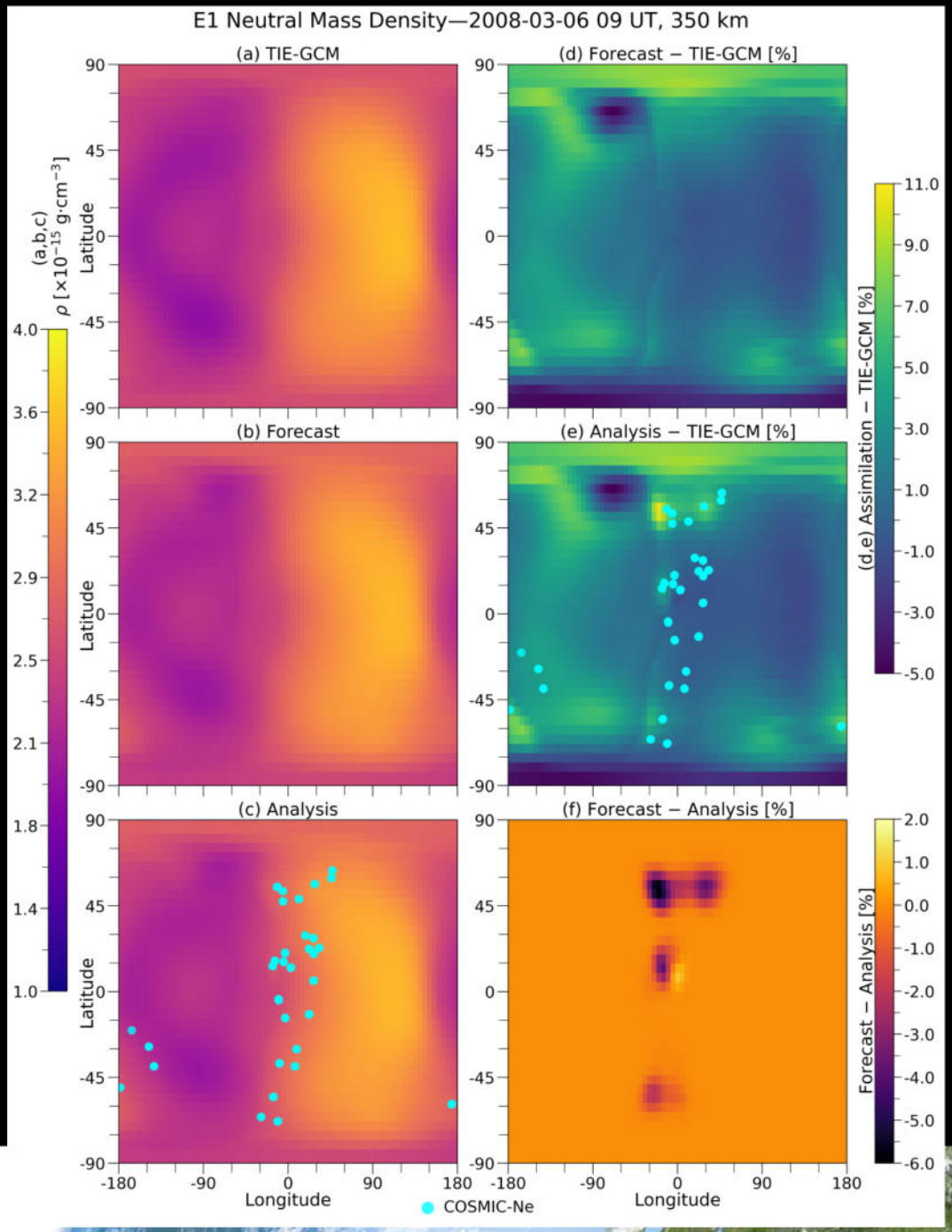
E1 Neutral Mass Density—2008-03-06 09 UT, 350 km
(a) TIE-GCM
(d) Forecast − TIE-GCM [%]
(b) Forecast
(e) Analysis − TIE-GCM [%]
(c) Analysis
(f) Forecast − Analysis [%]
(a,b,c) ρ [×10⁻¹⁵ g·cm⁻³]
(d,e) Assimilation − TIE-GCM [%]
Forecast − Analysis [%]
Latitude
Longitude
COSMIC-Ne

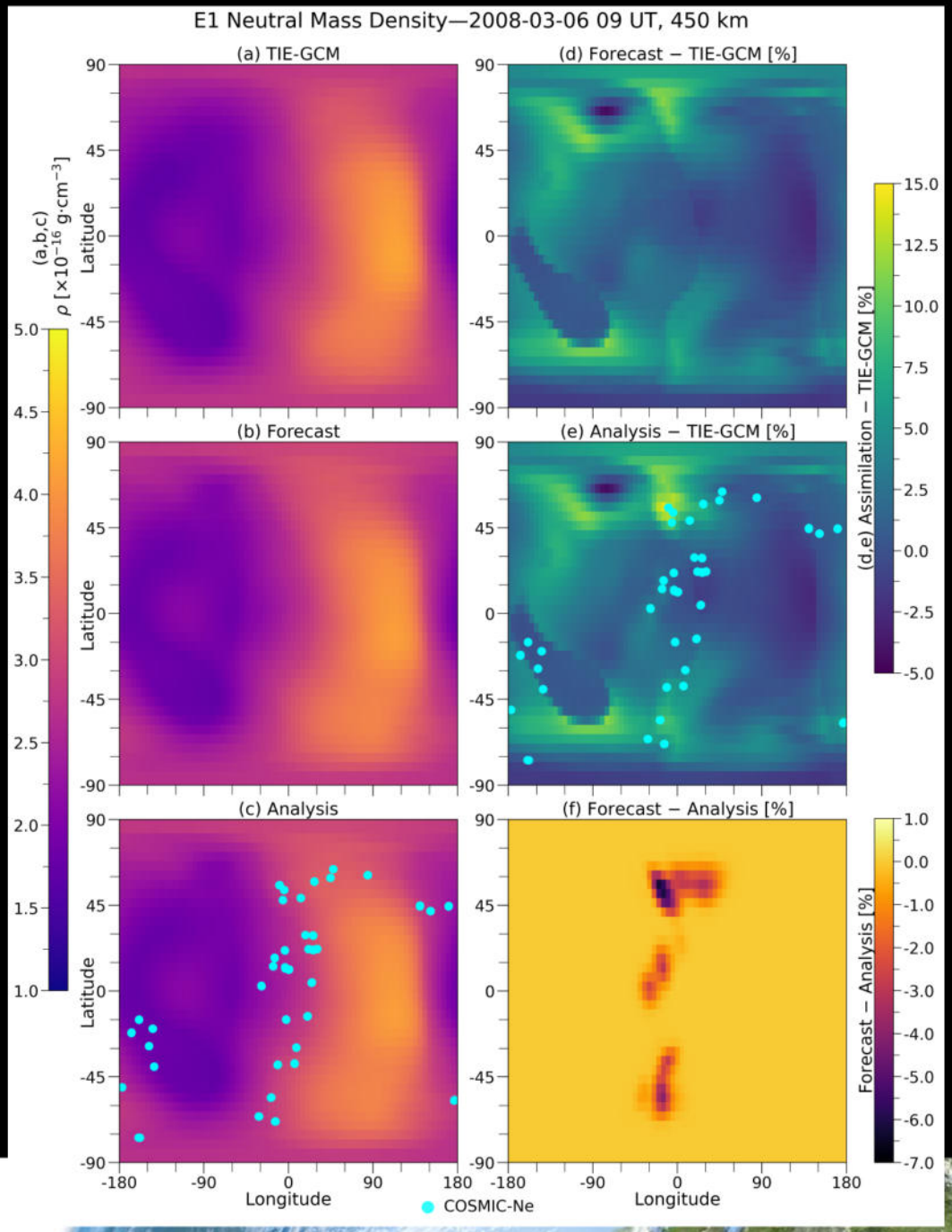
E1 Neutral Mass Density—2008-03-06 09 UT, 450 km
(a) TIE-GCM
(d) Forecast − TIE-GCM [%]
(b) Forecast
(e) Analysis − TIE-GCM [%]
(c) Analysis
(f) Forecast − Analysis [%]
(a,b,c) ρ [×10⁻¹⁶ g·cm⁻³]
(d,e) Assimilation − TIE-GCM [%]
Forecast − Analysis [%]
Latitude
Longitude
COSMIC-Ne

Same as above except for E2.

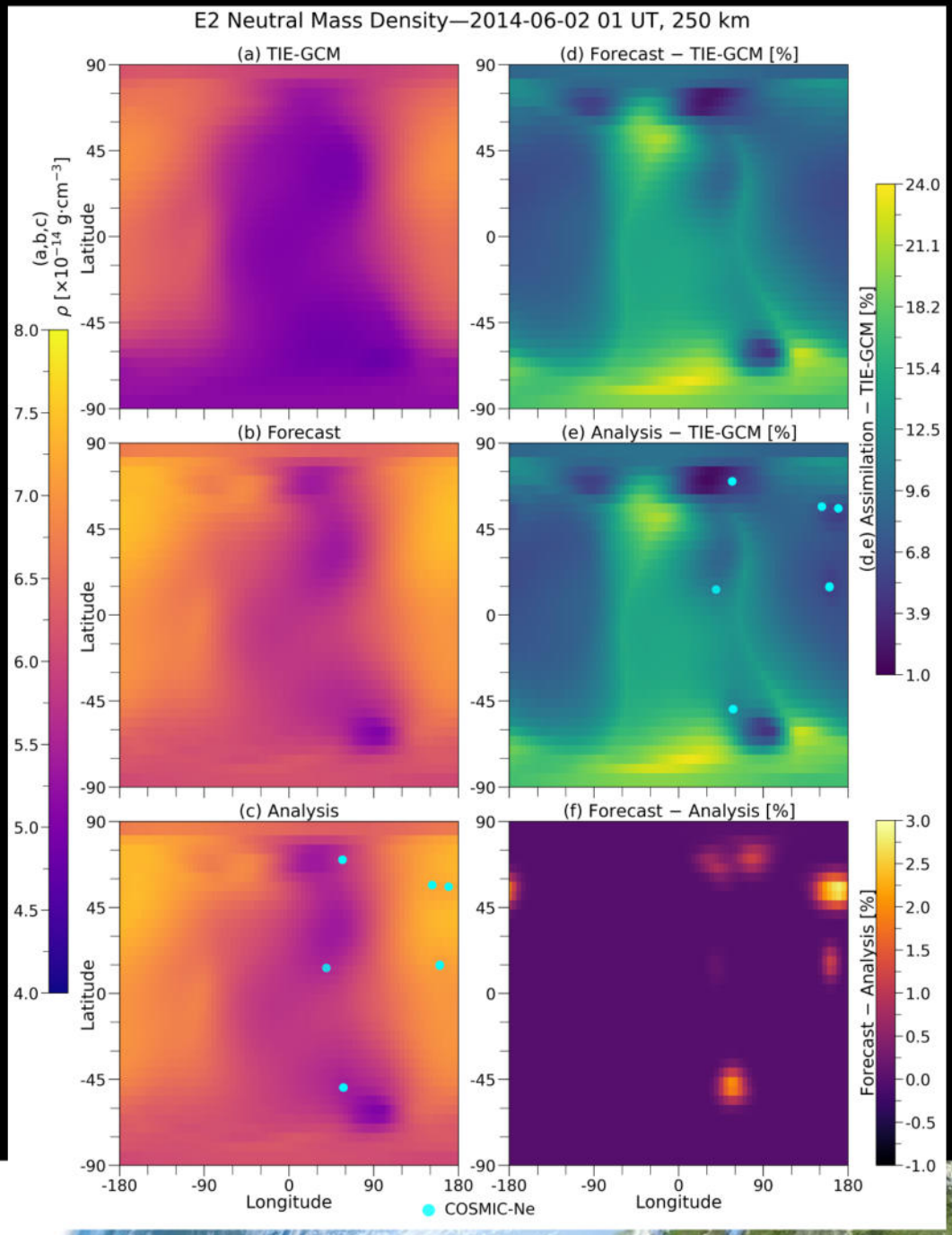
E2 Neutral Mass Density—2014-06-02 01 UT, 250 km
(a) TIE-GCM
(d) Forecast − TIE-GCM [%]
(b) Forecast
(e) Analysis − TIE-GCM [%]
(c) Analysis
(f) Forecast − Analysis [%]
(a,b,c) ρ [×10⁻¹⁴ g·cm⁻³]
(d,e) Assimilation − TIE-GCM [%]
Forecast − Analysis [%]
Latitude
Longitude
COSMIC-Ne

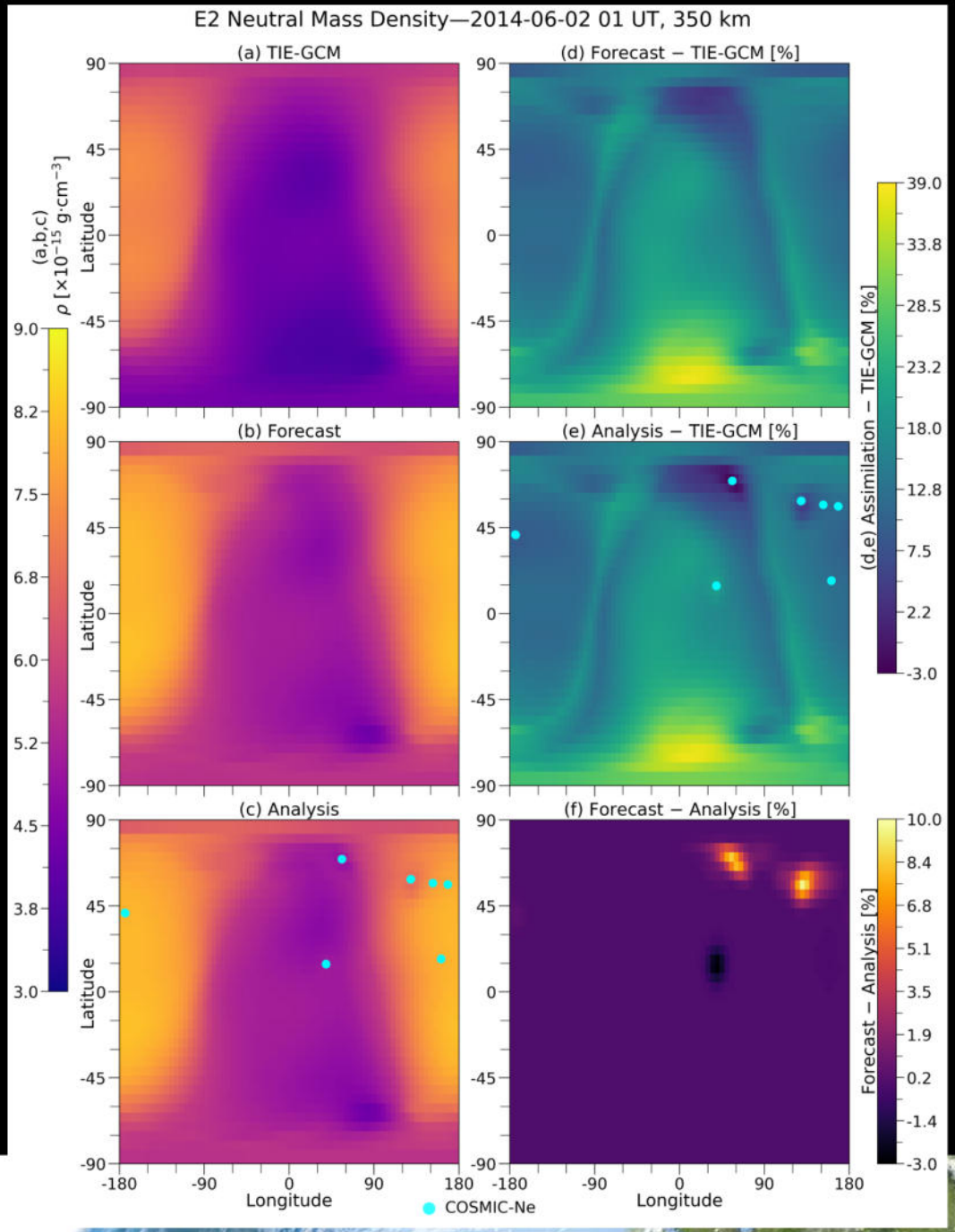
E2 Neutral Mass Density—2014-06-02 01 UT, 350 km
(a) TIE-GCM
(d) Forecast − TIE-GCM [%]
(b) Forecast
(e) Analysis − TIE-GCM [%]
(c) Analysis
(f) Forecast − Analysis [%]
(a,b,c) ρ [×10⁻¹⁵ g·cm⁻³]
9.0
8.2
7.5
6.8
6.0
5.2
4.5
3.8
3.0
(d,e) Assimilation − TIE-GCM [%]
39.0
33.8
28.5
23.2
18.0
12.8
7.5
2.2
-3.0
Forecast − Analysis [%]
10.0
8.4
6.8
5.1
3.5
1.9
0.2
-1.4
-3.0
Latitude
Longitude
90
45
0
-45
-90
-180
-90
0
90
180
COSMIC-Ne

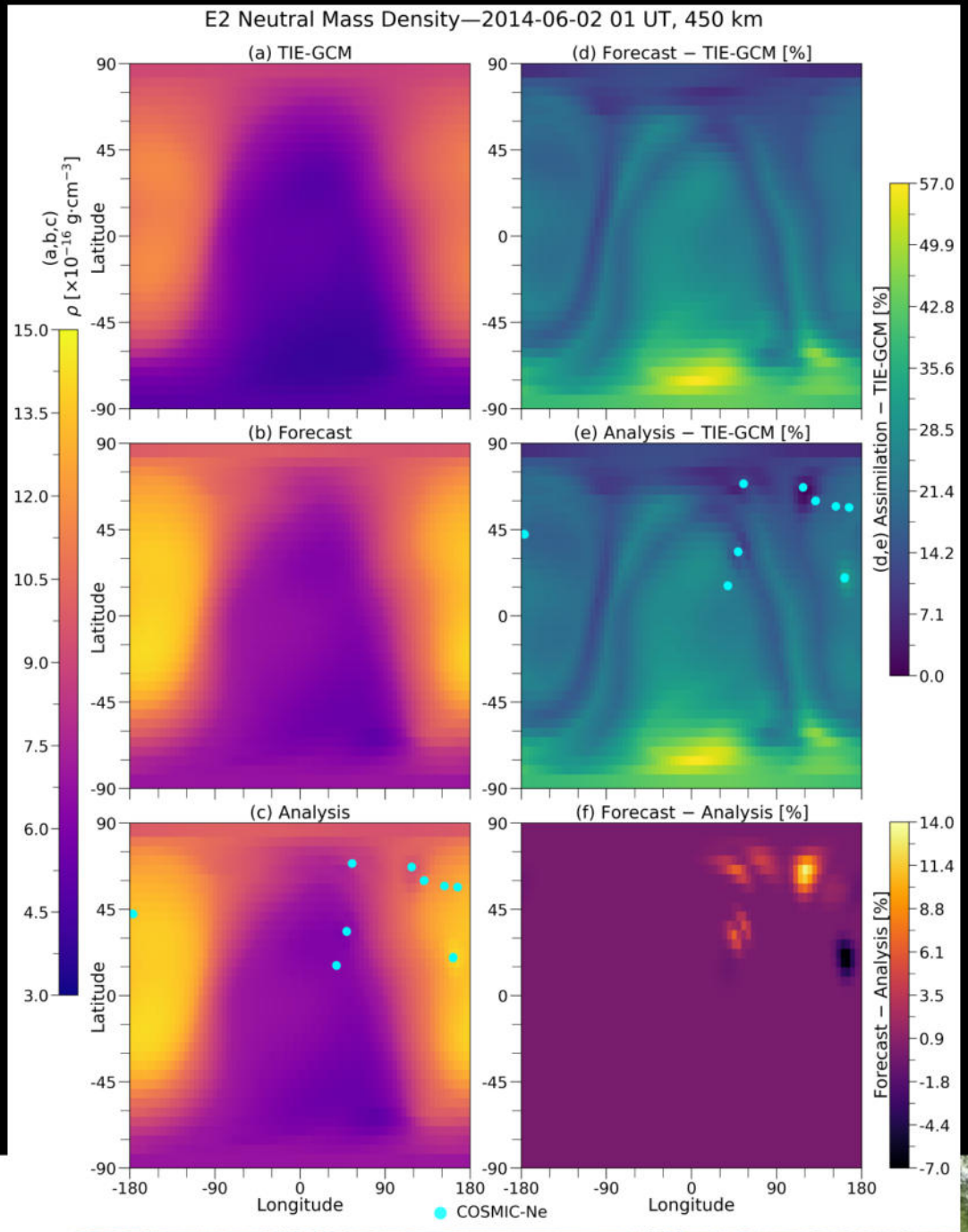
E2 Neutral Mass Density—2014-06-02 01 UT, 450 km
(a) TIE-GCM
(d) Forecast − TIE-GCM [%]
(b) Forecast
(e) Analysis − TIE-GCM [%]
(c) Analysis
(f) Forecast − Analysis [%]
(a,b,c) ρ [×10^−16 g·cm^−3]
(d,e) Assimilation − TIE-GCM [%]
Forecast − Analysis [%]
Latitude
Longitude
COSMIC-Ne

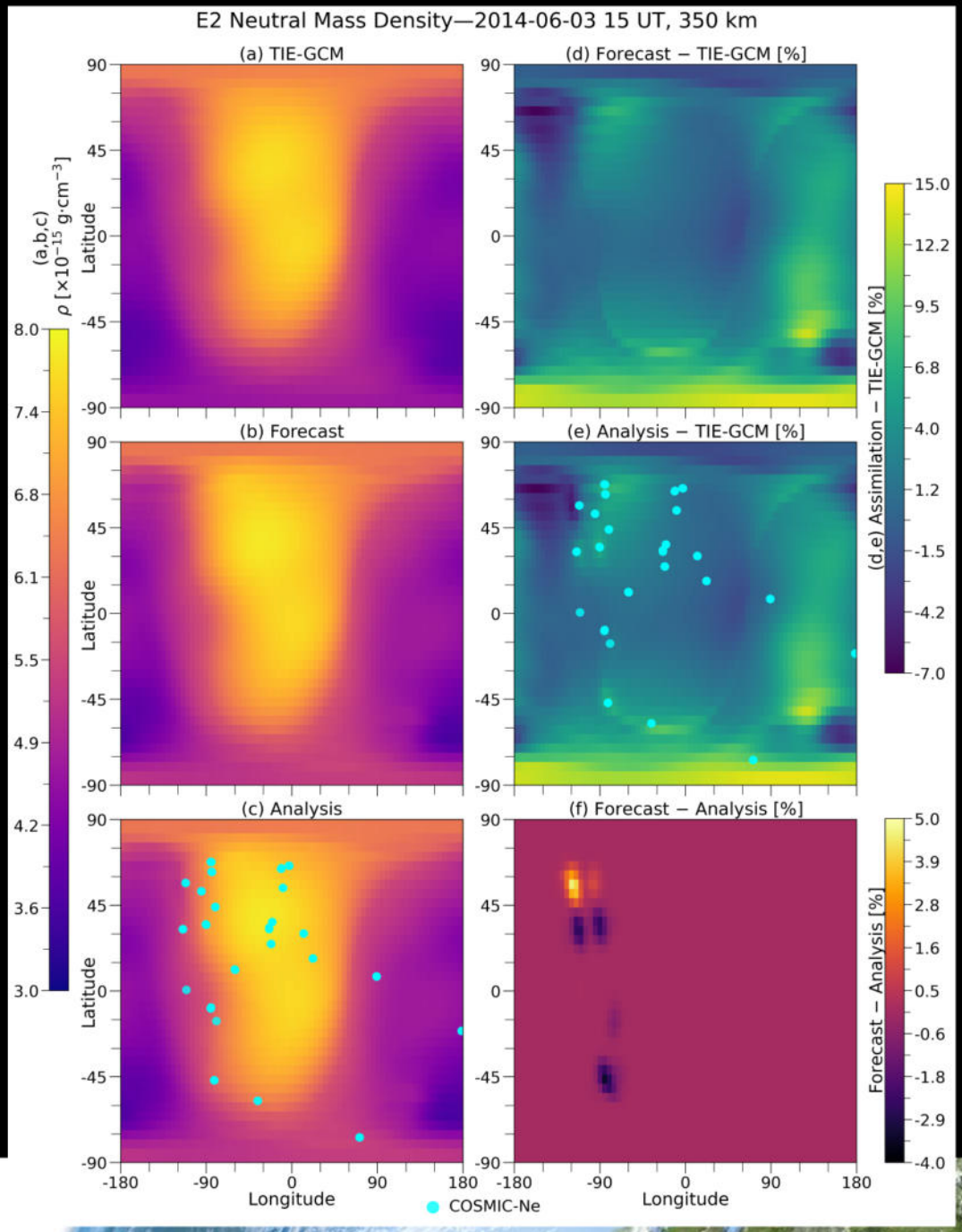
E2 Neutral Mass Density—2014-06-03 15 UT, 350 km
(a) TIE-GCM
(d) Forecast − TIE-GCM [%]
(b) Forecast
(e) Analysis − TIE-GCM [%]
(c) Analysis
(f) Forecast − Analysis [%]
(a,b,c) ρ [×10⁻¹⁵ g·cm⁻³]
8.0
7.4
6.8
6.1
5.5
4.9
4.2
3.6
3.0
(d,e) Assimilation − TIE-GCM [%]
15.0
12.2
9.5
6.8
4.0
1.2
-1.5
-4.2
-7.0
Forecast − Analysis [%]
5.0
3.9
2.8
1.6
0.5
-0.6
-1.8
-2.9
-4.0
Latitude
Longitude
90
45
0
-45
-90
-180
-90
0
90
180
COSMIC-Ne

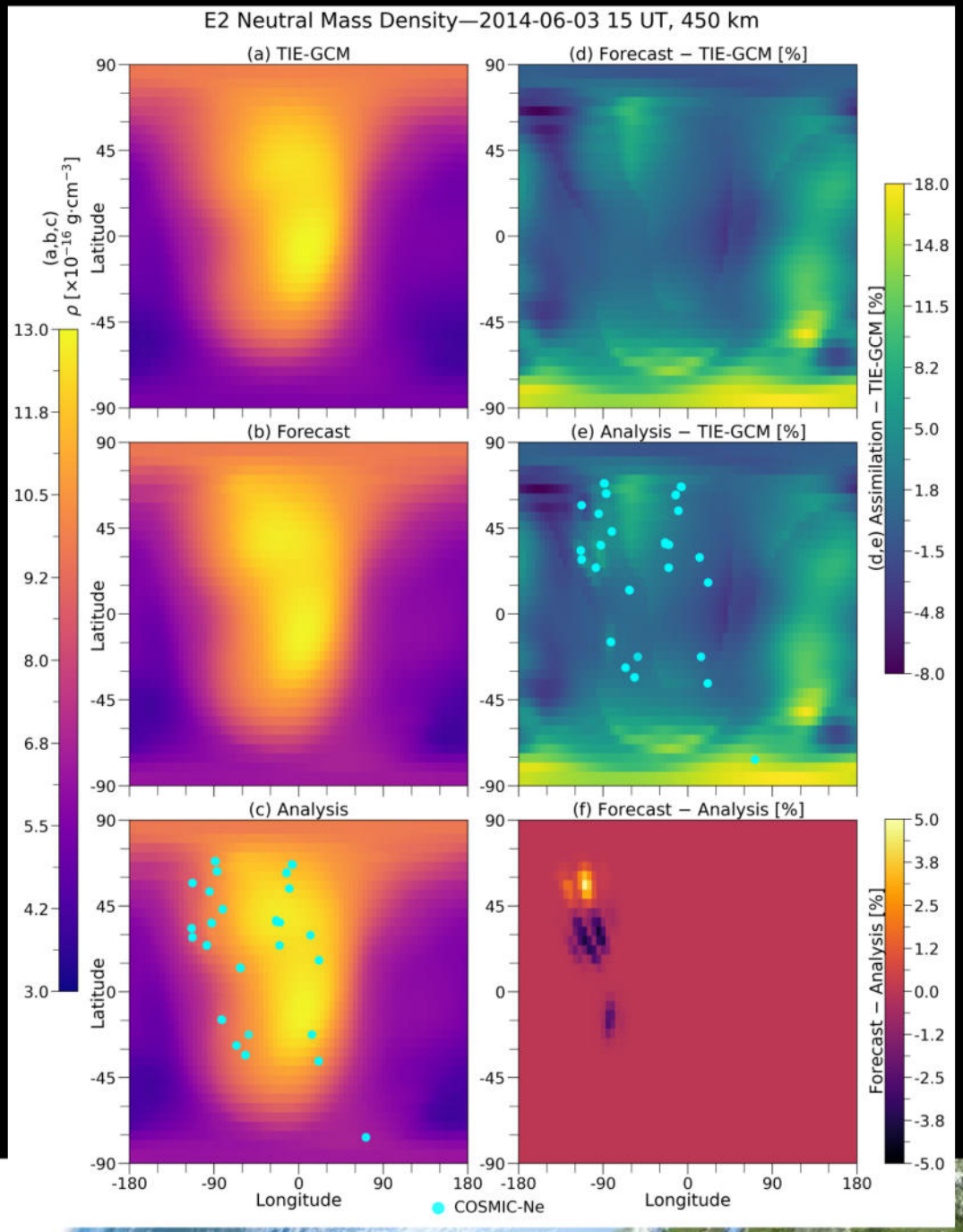
E2 Neutral Mass Density—2014-06-03 15 UT, 450 km
(a) TIE-GCM
(d) Forecast − TIE-GCM [%]
(b) Forecast
(e) Analysis − TIE-GCM [%]
(c) Analysis
(f) Forecast − Analysis [%]
(a,b,c) ρ [×10^−16 g·cm^−3]
(d,e) Assimilation − TIE-GCM [%]
Forecast − Analysis [%]
Latitude
Longitude
COSMIC-Ne

Summary and Conclusions

Above results correspond to two experiments of assimilating electron densities into TIE-GCM using the EnKF technique. The results demonstrated the capability of the assimilation technique in the presence of realistic data assimilation scenarios to forecast the highly dynamical thermosphere.

The comparisons in the observation-space showed that assimilation of COSMIC-*Ne* can significantly change the model state to be inline with the observations. This change is more pronounced in the E2 night-time electron density profiles than others. The number of COSMIC-*Ne* profiles available to assimilate significantly depends on latitude and local time.

The validation results showed that the COSMIC-*Ne*-guided ionosphere state outperforms the GPI-guided TIE-GCM.
The results also demonstrated that assimilation of electron density can significantly impact the neutral mass density estimates of the model.

./continued

The experiments E1 and E2 indicated that using COSMIC-*Ne* profiles in an operational-forecasting setting is challenging and that the area and local time coverages of the profiles are perhaps too sparse to be used in, for example, applications of orbit prediction.

The comparisons of neutral mass density may provide insights into the biases inherent in TIE-GCM—particularly along thermospheric features with sharp spatial gradients. The systematic biases that above results highlighted could be an indication that the specification of plasma-neutral interactions in TIE-GCM needs further adjustments.

The experiments mainly focused on the assimilation accuracy during different solar activity periods. More work needs to be done to identify and improve model bias due to external forcing. Assimilation of other thermospheric data, for example, atomic oxygen, thermospheric neutral winds and temperature could also help unravel some of the difficulties associated with forecasting thermospheric mass density.

References

- Heelis, R. A., J. K. Lowell, and R. W. Spiro (1982), A model of the high-latitude ionospheric convection pattern, Journal of Geophysical Research: Space Physics, 87(A8), 6339–6345, doi:10.1029/JA087iA08p06339.
- Hagan, M. E., R. G. Roble, and J. Hackney (2001), Migrating thermospheric tides, Journal of Geophysical Research: Space Physics, 106(A7), 12,739–12,752, doi:10.1029/2000JA000344.
- Qian, L., S. C. Solomon, and T. J. Kane (2009), Seasonal variation of thermospheric density and composition, Journal of Geophysical Research: Space Physics, 114(A1), doi:10.1029/2008JA013643.
- Richmond, A. D., E. C. Ridley, and R. G. Roble (1992), A thermosphere/ionosphere general circulation model with coupled electrodynamics, Geophysical Research Letters, 19(6), 601–604, doi:10.1029/92GL00401.
- Solomon, S. C., and L. Qian (2005), Solar extreme-ultraviolet irradiance for general circulation models, Journal of Geophysical Research: Space Physics, 110(A10), doi:10.1029/2005JA011160.